HHS Public Access

Author manuscript

Sci Immunol. Author manuscript; available in PMC 2024 June 30.

Published in final edited form as:

Sci Immunol. 2023 June 30; 8(84): eade5343. doi:10.1126/sciimmunol.ade5343.

Polymorphic KIR3DL3 expression modulates tissue-resident and innate-like T cells

William H. Palmer[1,2], **Laura Ann Leaton**[1,2], **Ana Campos Codo**[1,2], **Bergren Crute**[2], **James Roest**[3], **Shiying Zhu**[3], **Jan Petersen**[3], **Richard P. Tobin**[4], **Patrick S. Hume**[5], **Matthew Stone**[4], **Adrie van Bokhoven**[6], **Mark E. Gerich**[7], **Martin D. McCarter**[4], **Yuwen Zhu**[4], **William J. Janssen**[5], **Julian P. Vivian**[3], **John Trowsdale**[8], **Andrew Getahun**[2], **Jamie Rossjohn**[3,9], **John Cambier**[2], **Liyen Loh**[2,10,†], **Paul J. Norman**[1,2,†,*]

[1]Department of Biomedical Informatics, University of Colorado School of Medicine, Aurora, CO, USA

[2]Department of Immunology & Microbiology, University of Colorado School of Medicine, Aurora, CO, USA

[3]Infection and Immunity Program and Department of Biochemistry and Molecular Biology, Biomedicine Discovery Institute, Monash University, Clayton, Victoria, Australia

[4]Department of Surgery, Division of Surgical Oncology, University of Colorado School of Medicine, Aurora, CO, USA

[5]Department of Medicine, National Jewish Health, Denver, CO, USA

[6]Department of Pathology, University of Colorado School of Medicine, Aurora, CO, USA

[7]Division of Gastroenterology and Hepatology, University of Colorado School of Medicine, Aurora, CO, USA

[8]Department of Pathology, University of Cambridge, UK

[9]Institute of Infection and Immunity, Cardiff University, School of Medicine, Heath Park, Cardiff, UK

[10]Department of Microbiology and Immunology, University of Melbourne, at the Peter Doherty Institute for Infection and Immunity, Parkville, Australia

Abstract

[*]Correspondence: paul.norman@cuanschutz.edu.
† Authors contributed equally

Author contributions: WP, LAL, LL and PN conceived the study. WP, LAL, AC, BC, JP, RT, YZ, JV, AG, LL and PN designed experiments. WP, LAL, AC, BC, JRoe, SZ, JP and LL performed experiments. AG, JRos, JC, LL and PN supervised experiments. WP, LAL, AC, BC, JRoe, SZ, JP, LL and PN performed data analysis and visualization. WP, RT, PH, MS, AB, MG, MM, MJ, YZ, JV, JT, JRos, JC and PN provided material resources. JRos, LL and PN acquired funding. WP, LAL, LL and PN wrote the manuscript. All authors were involved in the critical review of the manuscript.

Competing interests: The authors declare they have no competing interests.

List of Supplementary Materials
Materials and Methods
Supplementary Figures S1–S11
Supplementary Tables S1–S5 (Excel Spreasheets)
MDAR Reproducibility Checklist

Most human killer cell immunoglobulin-like receptors (KIR) are expressed by natural killer (NK) cells and recognize HLA class I molecules as ligands. KIR3DL3 is a conserved but polymorphic inhibitory KIR recognizing a B7 family ligand, HHLA2, and is implicated for immune checkpoint targeting. The expression profile and biological function of KIR3DL3 have been somewhat elusive, so we searched extensively for KIR3DL3 transcripts, revealing highly enriched expression in γδ and CD8+ T cells rather than NK cells. These KIR3DL3 expressing cells are rare in the blood and thymus but more common in the lungs and digestive tract. High resolution flow cytometry and single cell transcriptomics showed that peripheral blood KIR3DL3+ T cells have an activated transitional memory phenotype and are hypofunctional. The TCR usage is biased towards genes from early rearranged TCR-α variable segments or Vδ1 chains. In addition, we show that TCR-mediated stimulation can be inhibited through KIR3DL3 ligation. Whereas we detected no impact of KIR3DL3 polymorphism on ligand binding, variants in the proximal promoter and at residue 86 can reduce expression. Together, we demonstrate that KIR3DL3 is upregulated alongside unconventional T cell stimulation, and that individuals may vary in their ability to express KIR3DL3. These results have implications for the personalized targeting of KIR3DL3/HHLA2 checkpoint inhibition.

One sentence summary

KIR3DL3 is an inhibitory receptor expressed by tissue-resident T cells, and has polymorphism affecting expression.

Keywords

KIR3DL3; HHLA2; B7H7; γδ T cells; CD8+ T cells; TCR; IEL; intestine; lung; polymorphism

Introduction

Detection and elimination of infected or cancerous cells by cytotoxic lymphocytes is vital for survival (1–3). In this role, alongside functions in placentation and tissue transplantation (4–8), killer cell immunoglobulin-like receptors (KIR) modulate the cytotoxic and inflammatory activity of human natural killer (NK) and some T cells (9, 10). Inhibitory KIR educate developing NK cells, enabling them to kill malignant or infected cells marked by altered expression of cell surface ligands, namely HLA class I molecules (9, 10). Expression of inhibitory KIR by T cells can also promote cell survival, dampen responses to T cell receptor stimuli, and suppress other auto-reactive T cells (11–15).

Among the 13 functionally distinct KIR molecules (16–18), KIR3DL3 is unusual. Whereas most *KIR* genes vary by presence and copy number (16), *KIR3DL3* is present in every individual across diverse populations and conserved among humans and catarrhine primates (19). *KIR3DL3* is also the most genetically diverse *KIR*, with a subset of polymorphic residues having genetic patterns consistent with the action of diversifying natural selection (19). Through recent high-throughput *in vitro* fusion protein microarray screening, KIR3DL3 was found to recognize the B7 family protein HHLA2 as a ligand (20, 21), contrasting other KIR that recognize HLA class I as ligands. HHLA2 expression by target cells coordinates inhibition of cytotoxic responses by KIR3DL3-transduced NK

cell lines (22, 23), consistent with the presence of an immunoreceptor tyrosine-based inhibitory motif (ITIM) in the KIR3DL3 cytoplasmic tail (19). These evolutionary patterns and ligand binding suggest an essential immunoregulatory function of KIR3DL3. However, the immunological role of KIR3DL3 remains unclear.

The lack of a described expression pattern for KIR3DL3 has been a considerable obstacle to understanding the biological importance of this inhibitory receptor. Most KIR are expressed stochastically and frequently by peripheral NK cells (11, 24, 25), but efforts to localize KIR3DL3 on peripheral NK cells have produced contradictory results. KIR3DL3 expression in peripheral blood, as assayed by PCR, was found to be undetectable in 80% of donors (26), and perhaps enriched in $CD56^{bright}$ peripheral blood and decidual NK cells (27). However, more recently, widespread KIR3DL3 expression was described in peripheral $CD56^{dim}$ NK cells (23), while another report showed induced cell surface expression in peripheral blood CD4+ and CD8+ T cells following *in vitro* TCR-mediated activation and long-term cell culture (22). Distinct transcription factor binding sites in the KIR3DL3 promoter support a distinct expression profile as compared to other KIR (28, 29). Altogether, the presently available data describing KIR3DL3 expression are incongruent, fragmented, and warrant a wide-ranging search for KIR3DL3 across tissues and cell types.

KIR3DL3 potentially represents an immune checkpoint, with the HHLA2-KIR3DL3 interaction suggested as an immunotherapeutic target. Other B7 family ligands and their receptors, such as PD-L1 and CTLA-4, have been the targets for successful immunotherapies (30, 31). Indeed, HHLA2 is upregulated in tumors of the lung, gastrointestinal tract, kidney, and liver, and in some cases, expression has been associated with poor prognosis (32–35). Given KIR3DL3 is an inhibitory receptor, expression on tumor infiltrating lymphocytes could lead to immune evasion by HHLA2+ tumors. Prerequisite to harnessing any medicinal utility is a basic characterization of KIR3DL3 expression and the function of its polymorphism. Given the high prevalence of functional polymorphism in other KIR proteins (36–41) and promoters (42, 43), a consideration of KIR3DL3 diversity is paramount to understanding the role of KIR3DL3 across human populations. In this study, we used a highly specific monoclonal antibody for KIR3DL3 in combination with multi-dimensional spectral flow cytometry and single cell transcriptomics, to decipher the tissue distribution of KIR3DL3, and its immunoregulatory function. Further, we determine functional consequences of selected promoter and amino acid polymorphism. These studies shed fundamental biological insight into this enigmatic KIR family member.

Results

KIR3DL3 RNA expression is found in cytotoxic lymphocytes from diverse tissues.

Although *KIR3DL3* expression is often silenced through promoter methylation, *KIR3DL3* mRNA has been identified previously in $CD56^{bright}$ cells from peripheral blood and decidua (26, 27). To better determine the extent of *KIR3DL3* transcription, we examined RNA sequencing experiments publicly available from the NCBI short read archive (SRA). By searching for a unique *KIR3DL3*-characterizing sequence (see Methods), we identified KIR3DL3 mRNA in 196 of the 360,787 available data sets. After excluding cell lines, *ex vivo* experiments and replicated individuals, we ultimately identified 84 individuals across

48 studies showing evidence for KIR3DL3 expression (Table S1). Of the 84 individuals, we did not observe any evidence for differences in expression levels (as determined by normalized read counts) of KIR3DL3 across ages, between males and females, between donors who were healthy or with disease, nor any interactions between age, sex, and health status (Table S1). However, 7 of 9 KIR3DL3+ samples from the lung, and an additional lung-draining lymph node sample (Table S1), were from individuals with non-small cell lung cancer, which is often marked by high HHLA2 expression (33). Thus, while we did not observe a general effect of health status on *KIR3DL3* mRNA expression, expression may still be enriched in specific malignant or immunopathological diseases.

Cell sorted cytotoxic lymphocytes derived from diverse tissues constituted the majority of samples positive for *KIR3DL3* mRNA (Fig. 1A; Table S1). Among these tissues, *KIR3DL3* transcripts were found most often in the digestive tract, lung, and lymphoid organs, with each of these systems being represented by multiple independent studies (digestive: 5; lung: 6; lymphoid: 4). We also identified KIR3DL3 transcripts from decidual T cells, consistent with previous reports of KIR3DL3 expression by $CD56^{bright}$ decidual NK cells (27). We observed sequence read coverage across all KIR3DL3 exons (Fig. 1B). Remarkably, the tissues identified as most likely to express KIR3DL3 (Fig. 1A,C) overlap considerably with HHLA2 protein expression patterns (44) (Fig. 1D), suggesting either KIR3DL3+ cells are recruited to these tissues, or KIR3DL3 is induced in ligand-rich microenvironments. In summary, we detected KIR3DL3 mRNA in peripheral blood mononuclear cells (PBMCs) and tissues from the respiratory, digestive, and lymphoid systems. We next sought to confirm that presence of full KIR3DL3 transcripts correlates with cell surface protein expression.

Cell surface KIR3DL3 is most frequently found in lung and the digestive tract tissues

Guided by the SRA data, we used multi-parameter spectral flow cytometry to delineate the specific lymphocyte subsets that express cell surface KIR3DL3 protein. Thus, we used single cell suspensions of PBMCs, lung, colon, and thymus tissues. The CH21 antibody specifically stains KIR3DL3 (27) (Fig. S1 for antibody specificity; Fig. S2 for gating strategy), and consistently identified a small yet distinct population of non-B cell lymphocytes among PBMCs (Median= 0.007%, n=13, $p < 0.001$, Fig. 2A–B, Fig. S3). In thymic tissues, KIR3DL3 expressing cells were found at a similar frequency as observed in peripheral blood (Median=0.006%, n=3, Fig. 2A–B). Consistent with SRA data (Fig. 1A–B), we found that the proportion of KIR3DL3+ cells was significantly higher in lung lymphocytes (0.04% of non-B lymphocytes; n=5, $p = 0.03$), colon intra-epithelial lymphocytes (IELs) (0.06%; n=3, $p = 0.04$), and small intestine IELs (0.45%; n=3 $p < 0.001$) as compared to peripheral blood (Fig. 2B). We did not observe any correlation between the frequency of KIR3DL3+ cells with either sex ($p = 0.49$) or age ($p = 0.16$). These results confirm that SRA data reflects the protein expression of KIR3DL3, which occurs more frequently in lymphocytes of mucosal tissues.

KIR3DL3 is expressed in CD8+ and γδ T cells of peripheral blood and tissues.

To specifically phenotype the lymphocyte subsets that express KIR3DL3, we performed multi-parameter flow cytometry on peripheral blood and tissue-derived immune cells. We ensured accurate co-expression of phenotypic markers on the rare KIR3DL3+ lymphocyte

population by enriching for KIR3DL3+ cells using a magnetic bead-based method. Specifically, anti-PE microbeads bound to CH21 and secondary anti-Ms-PE (Fig. 2A). We assessed significance using binomial models, thereby considering any uncertainty that may be caused by a small number of observations. We then calculated NK and T cell subset frequencies in all CD19- (i.e. background), CD19-KIR3DL3+, or CD19-KIR3DL1+ lymphocytes (Fig. 2C) and determined enrichment of these T/NK cell subsets in either KIR3DL1+ (Fig. 2D) or KIR3DL3+ (Fig. 2E) cells, as compared to the background frequency. Both KIR3DL1 and KIR3DL3 were significantly less likely to be expressed by CD4+ T cells ($p<0.001$) and KIR3DL1 expression was highly enriched on NK cells ($p < 0.001$), as expected (Fig 2D–E). Strikingly, across PBMC and tissues, KIR3DL3 was most enriched on γδ T cells ($p <0.001$), followed by CD8+ T cells ($p = 0.002$) (Fig. 2E). In PBMCs, while the median proportion of γδ T cells of CD19- peripheral lymphocytes was 2.1%, 16.3% of KIR3DL3+CD19- cell lymphocytes were γδ T cells. KIR3DL3+ lymphocytes of the lung, small intestine, and colon mirrored these patterns, with KIR3DL3 expression enriched in lung CD8+ T cells (lung: $p = 0.06$) and in lung, colon, and small intestine γδ T cells (lung: $p = 0.002$; colon: $p = 0.08$; sm. Intestine: $p = 0.006$). The absolute frequency of KIR3DL3 expression was most striking in digestive tract IELs, where an average of 14% (range: 0.3%−58%) of γδ T cells expressed KIR3DL3 (Fig. 2F, Fig. S4). Although a recent report showed extensive expression of KIR3DL3 by peripheral blood NK cells (23), our data indicate that finding was due to cross reactivity of the monoclonal antibody with KIR3DL1 (Fig. S1), which can be expressed by a significant proportion of NK cells (25). KIR3DL3 is therefore not principally an NK cell receptor but likely a tissue resident T cell marker.

Previous studies have shown that KIR can be expressed on the cell surface of terminally differentiated CD8+ T cells (11). To determine the differentiation and memory phenotypes of KIR3DL3+ T cells across the tissues, we analyzed the cell surface markers CD27 and CD45RA in combination, thus deriving subsets of naïve-like (CD27+CD45RA+), central memory-like (CM, CD27+CD45RA-), effector memory-like (EM, CD27-CD45RA-), and EM re-expressing CD45RA (EMRA, CD27-CD45RA+)-like T cells. As above, we compared background CD8+ or γδ T cells to KIR3DL1+ or KIR3DL3+ T cells to determine if these KIR are preferentially expressed in certain T cell subsets. Most notably, we observed preferential KIR3DL3 expression on $CD27^{hi}$ cells, with greater CD27 mean fluorescent intensity (MFI) as compared to background naïve or CM populations (Fig. 3A). Interestingly, KIR3DL3+ γδ T cells of peripheral blood and lung were significantly more likely to co-express CD27 and CD45RA (PBMC, $p = 0.014$; lung, $p = 0.046$), suggestive of a naïve-like phenotype (Fig. 3A–B; Fig. S5). KIR3DL3+ CD8+ T cells were distributed across all four differentiation states, with significantly less EM-like subsets in PBMCs (Fig. 3B, $p=0.042$). Conversely, KIR3DL1 expression on PBMCs was preferentially enriched in CD8+ EMRA T cells (Fig. 3B, $p = 0.014$), although this enrichment did not exist in γδ subsets (Fig. 3B, $p = 0.52$). Importantly, KIR3DL3 and KIR3DL1 expression were not significantly correlated. Consistent with the mature nature of IELs, we observed that almost all colon and small intestine IELs were EM or EMRA-like, including KIR3DL3+ cells (Fig. 3B).

Because the KIR3DL3+ T cells were observed to have a “naïve-like” (CD27+CD45RA+) phenotype, we tested if they also co-express the CCR7 and CD62L molecules important for homing to lymph nodes. Whereas naïve-like CD8+ T cells tended to co-express CCR7 and CD62L, naïve-like γδ T cells did not. In comparison, CD8+ T and γδ T cells that expressed KIR3DL3 were less likely to express CD62L and CCR7, resembling naïve-like γδ T irrespective of their TCR type (Fig. 3C–D). Consistent with a lack of lymphoid homing markers, we observed only 0.001% of T cells present in a healthy mesenteric lymph node expressed KIR3DL3, in comparison to 0.1% of T cells from associated colon tissue of the same donor (Fig. 3E).

Analyses of tissue residency markers and CD56, constitutively expressed on NK cells and populations of cytotoxic and innate-like T cells (45), revealed an altered expression of CD56 and CD49a on KIR3DL3+ T cells. KIR3DL3+ CD8+ T cells had greater expression of CD56 in the thymus ($p=0.003$), lungs ($p=0.031$), and digestive tract ($p=0.001$), compared to KIR- cells (Fig. 3F). Although KIR3DL3+ γδ T cells had similar trends in CD56 expression to KIR3DL3+ CD8+ T cells, significant upregulation was only observed in the thymus (Fig. 3G, $p=0.03$). In comparison, KIR3DL1+ CD8+ T cells, had higher CD56+ than KIR- cells in PBMCs ($p<0.001$), in addition to all other tissues (lung, $p = 0.01$; IEL, $p=0.05$), with the exception of thymus, where there was little detectable expression of KIR3DL1. In most tissues, we did not observe differential expression of tissue residency markers CD103 and CD49a in KIR3DL3+ or KIR3DL1+ cells. The exception was in IELs, where a subset of KIR3DL3+ CD8+ T cells had a $CD49a^{hi}$ phenotype (Fig. 3 H–I, $p=0.03$).

Transcriptome data suggests KIR3DL3 is expressed by T cells from diverse tumors (Table S1). To confirm this observation, we investigated KIR3DL3 expression on tumor-infiltrating lymphocytes (TILs) from metastatic melanoma (Fig. S6). In three patients, we observed KIR3DL3 expression on tumor-infiltrating T cells (n=5, Fig. S6A–B) and at a higher frequency than observed in peripheral blood of healthy individuals (Fig. 2B). KIR3DL3+ TILs were primarily CD8+ T cells and co-expressed PD-1 and CD49a (Fig. S6C–D), suggesting an activated, tissue-resident phenotype (46).

In summary, KIR3DL3 expression is enriched in CD8+ T and γδ T cells across tissues, is co-expressed with CD27 in PBMC and lungs, and in more mature (i.e. CD27-), tissue-resident T cell subsets in digestive tract IELs.

KIR3DL3+ T cells have an altered effector cell transcriptional profile.

To characterize the determinants of KIR3DL3 expression to higher resolution, we performed scRNA sequencing on sorted populations of KIR3DL3+ PBMCs, alongside NK, CD8+ T, and γδ T cells, from five donors. We obtained transcriptomic data for 9,188 NK, 2,750 CD8+ T, 3,490 γδ T, and 1,050 KIR3DL3+ cells. Using Seurat, (47) we identified 9 distinct NK and T cell clusters (Fig. 4A), with KIR3DL3+ cells corresponding to a specific subpopulation of cells (Fig. 4B). Multimodal reference mapping of gene expression profiles to a CITE-seq dataset of immune cells from peripheral blood (47) suggested KIR3DL3+ cells have a transcriptional profile intermediate between canonical naïve and memory cell populations (Fig. 4C). KIR3DL3+ cells were nominally defined as EM CD8+ T cells, converse to their designation as naïve-like or CM-like by cell surface staining for CD27 and

CD45RA (Fig. 3B). To quantify the naïve state of KIR3DL3+ cells, we used VISION (48) to calculate a naïve T cell score, using markers that defined naïve T cells in our data. Indeed, we observed that KIR3DL3+ T cells were more transcriptionally naïve than background EM or γδ T cell subsets ($p<0.001$; Fig. 4D). Differential gene expression analysis (Table S2) revealed that this intermediate phenotype was due to the simultaneously low expression of genes encoding cytotoxic granule proteins (*PRF1*, *NKG7*, *GZMA, GZMB, GZMH, FGFBP2*) and those involved in protein translation (*EEF1A1*) and ribosomal biogenesis (*RPS8, RPS6, RPL34, RPL39, RPL31, RPS4X, RPS13, RPL3*) (Fig. 4E). Intracellular staining of PBMCs and analysis by flow cytometry agreed with the transcriptional profile, where reduced GzmB, GzmK, and Perforin protein expression was found in KIR3DL3+ CD8+ T and γδ T cells compared to total EM, CM or γδ T cells (Fig. 4F). Low expression of ribosome biogenesis genes is correlated with poor T cell proliferative capacity (49). To confirm KIR3DL3+ T cells have an altered proliferative capacity, we stimulated T cells in PBMC (n=11 donors) using magnetic beads covalently labeled with anti-CD3 and anti-CD28 to engage the TCR complex. Following 7 days, the absolute number of stimulated T cells expanded by 3.4-fold as compared to non-stimulated controls (Fig. 4G). Conversely, the expansion of KIR3DL3+ T cells was significantly muted (1.6-fold, $p < 0.001$) (Fig. 4G). Upregulation of CD25 was also significantly reduced in KIR3DL3+ T cells, as compared to KIR3DL3- T cells ($p = 0.002$, Fig. S7A). KIR3DL3+ T cells also demonstrated moderate responsiveness to IL-15 (Fig. S7B), suggesting an ability for TCR-independent activation.

As such, KIR3DL3+ T cells are an anomaly along the ‘innateness’ gradient (49), which proposes the gradual gain of effector function concomitant with the loss of proliferative capacity through reduced ribosome biogenesis. Instead, KIR3DL3 expression may mark a hyporesponsive T cell population with limited naïve-like effector function, but an effector-like proliferative capacity. Given the expression of naïve protein markers (CD45RA, CD27), loss of lymph node homing markers (CD62L, CCR7), and a transcriptional profile intermediate to canonical naïve and effector programs, we suggest KIR3DL3+ T cells may be described as having a transitional memory phenotype (50).

TCR-responsive genes define KIR3DL3+ T cells.

The most significantly upregulated gene among KIR3DL3+ CD8+ and γδ T cells was the TCR-inducible *FOS*, as compared to KIR3DL3- CD8+ ($p = 2.5\times10^{-75}$) and γδ T ($p = 4.7\times10^{-14}$) cells, respectively (Fig. 4E, Table S2). Indeed, the most highly induced genes included many known to be upregulated following TCR stimulation (e.g. JUN, FOSB, IL2RB, DUSP2, EGR1) (51, 52). To test the degree with which KIR3DL3+ cells were enriched for upregulation of TCR-responsive genes, we again used VISION to compute an integrated TCR activation score, using an unbiased set of established TCR-responsive genes (51, 52) (Fig. S8A). We found that KIR3DL3+ CD8 and γδ T cells had a significantly greater TCR activation score as compared to their KIR3DL3- counterparts (Fig. 4H–I). Consistent with recent TCR stimulation, we also observed reduced CD3 MFI on KIR3DL3+ T cells (Fig. 4J–K). Analyses of the recent activation and tissue resident memory marker, CD69, in PBMC and lung lymphocytes revealed that both KIR3DL3+ CD8+ (PBMC, $p<0.001$; lung, $p<0.001$) and γδ (PBMC, $p<0.001$; lung, $p<0.001$) T cells expressed higher proportions of CD69+ compared to their KIR3DL3- counterparts (Fig. 4L–N). Differences

in either CD3 MFI or frequency of CD69+ cells were not observed in KIR3DL1+ T cells (Fig. 4K,M-N). The majority of digestive tract IELs were CD69+, with no differences across KIR- or KIR+ T cells, consistent with a tissue resident profile. KIR3DL3+ thymocytes also were more likely to express CD69, CD27, and be CD4+CD8+, markers consistent with recent positive thymic selection (Fig. S8B–C).

Given the hyporesponsive transcriptional profile of KIR3DL3+ T cells, their muted proliferation in response to TCR-mediated stimulation, and reduced cytolytic molecules, we hypothesized KIR3DL3 is expressed as an immune checkpoint in auto-reactive T cells. Such cells may experience agonistic selection or chronic T cell stimulation. Gene set enrichment analyses (53) identified NF-κB targets as the most significantly upregulated gene set in KIR3DL3+ cells (CD8 $p^{adj} = 0.002$; γδ $p^{adj} = 0.02$), alongside downregulated metabolism genes such as those involved in oxidative phosphorylation (CD8 $p^{adj} = 0.006$; γδ $p^{adj} = 0.17$) or mTOR targets (CD8 $p^{adj} = 0.08$; γδ $p^{adj} = 0.03$). Both NF-κB and mTOR are required for sustained T cell activation (54) and oxidative phosphorylation can be reduced in T cells exhausted by chronic antigen stimulation (55). In summary, the transcriptional profile of KIR3DL3+ T cells is consistent with recent TCR stimulation, but without progression into an effector program.

KIR3DL3 is enriched on Vδ1+ γδ T cells and CD8+ T cells with early-rearranging TCR-α chains.

KIR3DL3 is expressed by both γδ and CD8+ T cells (Fig. 2) although, transcriptionally, they are distinct from conventional naïve and effector/memory T cell subsets (Fig. 4B). To understand whether the TCR repertoire of KIR3DL3+ T cells is clonally restricted or diverse, we performed single cell paired VDJ sequencing of the α and β or γ and δ TCR chains. We obtained paired TCR chain sequences from a total of 1,695 CD8+ αβ T cells, 1,252 γδ T cells, 399 KIR3DL3+ CD8+ αβ T cells, and 66 KIR3DL3+ γδ T cells. Diverse αβ V gene pairing was observed in KIR3DL3+ CD8+ T cells (Fig. 5A), with CDR3 diversity similar between KIR3DL3+ and KIR3DL3- αβ T cells (α-chain, p=0.7; β-chain, p=0.8). Strikingly, we observed that KIR3DL3+ γδ repertoire was dramatically altered as compared to the total γδ TCR repertoire (Fig. 5B–C). Vγ9Vδ2 are the most common subset of γδ T cells in peripheral blood, generated during gestation (56). KIR3DL3 expression was identified only rarely on these cells, instead being preferentially expressed in Vδ1 and to a lesser extent, Vδ3 γδ T cells (Fig. 5C). To confirm Vδ usage across tissues, we stained KIR3DL3+ T cells from peripheral blood, lung, thymus, and intestinal IELs with Vδ1 and Vδ2 specific antibodies (Fig. S2). Indeed, for KIR3DL3+ γδ T cells, the proportion of Vδ1+ is enriched over Vδ2+ cells in peripheral blood, and lungs (Fig. 5D–F). KIR3DL3+ γδ T cells were almost exclusively Vδ2-, in contrast to KIR3DL1+ γδ T cells which expressed either Vδ1 or Vδ2 (Fig. 5E–F). Likewise, in the thymus KIR3DL3+ γδ T cells were also Vδ1+ with negligible Vδ2 expression (Fig. 5G).

In the CD8+ KIR3DL3+ αβ T cells, when considering each TRAV or TRBV gene individually, TRAV41 was the only gene significantly enriched (Fig. 5C). Interestingly, TRAV41 gene usage defines an innate T cell population in some mammals (57) and in humans is in the most proximal 3’ gene position of the TRAV region. The latter is

noteworthy because innate-like CD8αα+ T cells enriched in intestinal tissues likely develop by thymic agonistic selection marked by early TCR-α gene re-arrangement (58–61). Early TCR-α rearrangement preferentially utilizes the TRAV and TRAJ genes that are closest in proximity, with TRAV41 in closest proximity to the TRAJ cluster. We therefore tested whether TRAV and TRAJ gene usage in KIR3DL3+ CD8+ T cells were biased towards early rearranging TCR-α chains. Indeed, we observed preferential usage for 3' TRAV ($p < 0.001$) and 5' TRAJ ($p < 0.001$) (Fig. 5H). While TRAV41 was most enriched in KIR3DL3+ αβ T cells, the effect was still significant with this gene removed (Fig. 5H, $p = 0.02$). Agonist-selected CD8αα+ tissue-resident T cells fail to downregulate *TRGC*, express Hobit, a transcription factor that coordinates tissue-residency and innate T cell phenotypes, and Helios, which can be induced upon strong TCR stimulation (58, 62). We observed upregulation of *TRGC2*, *ZNF683* (Hobit), and *IKZF2* (Helios) in KIR3DL3+ αβ T cells (Fig. 5I). Additionally, KIR3DL3+CD8+ T cells of peripheral blood and jejunum exhibited a reduced ratio of CDβ:CD8α, which has been described as an indicator of CD8αα expression in humans (63) (Fig. 5J). Together, these results suggest that KIR3DL3+ CD8+ T cells may represent a population of agonist-selected T cells.

KIR3DL3 binds HHLA2 to inhibit TCR signaling

To confirm that KIR3DL3 is an inhibitory receptor, we transduced the NKL cell line with KIR3DL3*003 containing a C-terminal FLAG tag (NKL-KIR3DL3^{FLAG}) and treated cells with the phosphatase inhibitor, pervanadate, to induce tyrosine phosphorylation (Fig. 6A). After pervanadate treatment, we precipitated KIR3DL3^{FLAG} using an anti-FLAG antibody and observed tyrosine phosphorylation and the co-immunoprecipitation of SHP-1 and SHP-2 (Fig. 6B). Recruitment of both SHP-1 and SHP-2 underlie inhibition by KIR3DL1 and other inhibitory KIR (64–66), suggesting KIR3DL3 functions with a similar mechanism.

To determine the ability of KIR3DL3 to inhibit TCR activity, we performed an *in vitro* calcium mobilization assay using a γδ TCR+ Jurkat T cell (67) transduced to express KIR3DL3*003 (Jurkat.9C2-KIR3DL3). Here, TCR signaling was induced by avidin crosslinking following loading of Jurkat.9C2-KIR3DL3 cells with biotinylated anti-CD3, with or without biotinylated anti-KIR3DL3 (CH21). TCR activity was measured by intracellular Ca^{2+} mobilization and Indo-1 staining. In this assay, co-aggregation of biotinylated-CH21 with biotinylated-anti-CD3 significantly reduced Ca^{2+} mobilization ($p < 0.05$; Fig. 6C, Fig. S9A). We confirmed this effect using a KIR3DL3-expressing IIA1.6 mouse B cell line, an established model for antigen receptor signaling. We stimulated IIA1.6 cells by crosslinking the BCR with biotinylated Fab anti-IgG and avidin, which induced intracellular Ca^{2+} as evidenced by Indo-1 staining (Fig. S9B). Co-recruitment of KIR3DL3 using biotinylated CH21 significantly reduced Ca^{2+} mobilization ($p < 0.05$).

We next aimed to confirm that KIR3DL3 can directly recognize the HHLA2 ligand. We recombinantly expressed both molecules and conducted surface plasmon resonance (SPR) experiments, where the HHLA2 ligand was the analyte and KIR3DL3 coupled to the streptavidin sensor chip. KIR3DL3 bound to HHLA2 with an affinity value (K_D) of 48.9μM (Fig. 6D), which is an affinity within the range observed for KIR3DL1 interacting with its HLA cIass I ligands (37).

To further validate and extend these observations, we utilized a Jurkat NFAT reporter system(68) stably expressing KIR3DL3. Jurkat-NFAT-Luc-KIR3DL3 cells were cultured with target CHO cells expressing membrane-bound αCD3 (CHO-αCD3)(68), with or without co-expression of HHLA2. Using this model, both the parental and KIR3DL3 Jurkat cells were activated in the presence of CHO-αCD3 cells (Fig. 6E). As previously observed(22), the interaction of KIR3DL3 with HHLA2 inhibited NFAT activity ($p < 0.001$), and blockade of the KIR3DL3 signal with the 26E10 blocking antibody restored NFAT signaling ($p < 0.001$) (Figure 6E). Therefore, KIR3DL3 binds HHLA2 to inhibit antigen receptor signaling, likely through ITIM phosphorylation and SHP recruitment.

KIR3DL3 polymorphism having distinct population genetic patterns does not impact ligand binding.

KIR polymorphism can drastically alter receptor expression, ligand recognition, and signaling function (8, 69, 70). As the KIR3DL3-HHLA2 interaction has potential as an immunotherapeutic target (22), the identification of functional KIR3DL3 polymorphism could inform patient selection and expected responses to treatment. We therefore aimed to test a panel of naturally occurring KIR3DL3 variants for their ability to alter KIR3DL3 function or expression. We chose to use the NKL line because the specific lysis readout is a well-established model for understanding polymorphic receptor-ligand interactions (71, 72). Indeed, we confirmed previous observations (22, 23) that HHLA2 expression in target cells specifically inhibits lysis by KIR3DL3+ effector NK cells (Fig. 6F), suggesting this system could be leveraged to study KIR3DL3 polymorphism.

Because functional variant sites are expected to have been the target of natural selection (40, 73), we focused on polymorphism previously identified at residues with signatures of diversifying natural selection (19). We created NKL lines expressing KIR3DL3 with the single residue changes in the D1 domain (R145H, R145S, I147V), transmembrane domain (Y300H, A303V), and cytoplasmic domain (A327P) (Fig. 6G). Each line expressing a KIR3DL3 variant was retrovirally transduced and, alongside a control “WT” KIR3DL3*003 allele, used in HHLA2-Fc binding assays and cytotoxicity assays. We incubated NKL, NKL-3DL3*003, and each KIR3DL3 variant line (excluding 327P, in the cytoplasmic domain) with HHLA2-Fc and observed KIR3DL3+ cells bound HHLA2-Fc across the variants, with minimal binding to NKL alone (Fig. 6H). We then incubated each transduced NKL line with 221 or 221-HHLA2 target cells, in each case comparing to the matched KIR3DL3*003 control line. The polymorphic residues tested did not significantly alter HHLA2-mediated inhibition (Fig. 6I).

KIR3DL3 polymorphism can alter cell surface expression and proximal promoter activity.

In addition to ligand binding, KIR polymorphism can reduce receptor expression at the cell surface (5, 8). To determine if the KIR3DL3 expression level can be determined by genetic variants, we considered polymorphisms at conserved protein residues and in transcription factor binding sites of the proximal promoter. We noticed that the KIR3DL3*039, *052, *059, and *069 allotypes are defined by a serine to proline change at position 86 (86P). This SNP (rs374399247) is rare in most populations but can be as common as 3.5% in certain African populations (74). Position 86 is also variable in KIR3DL1, where a serine to leucine

mutation results in reduced cell surface expression of the KIR3DL1*004 allotype (75). We compared KIR3DL3*039 expression to that of KIR3DL3*003 by transfecting 293T cells with C-terminal (intracellular) FLAG tagged KIR3DL3. Whereas levels of intracellular FLAG were similar between KIR3DL3*003 and KIR3DL3*039, extracellular KIR3DL3 staining using CH21 showed markedly reduced cell surface expression of KIR3DL3*039 (Fig. 6J). Specifically mutating residue 86 of KIR3DL3*003 to proline reproduced the reduced cell surface expression of KIR3DL3*039 (Fig. 6J), suggesting polymorphism at this position has similar effects in KIR3DL3 as KIR3DL1.

The intermediate and proximal promoter regions have been characterized for *KIR3DL3* (28, 76). Promoter polymorphism in other *KIR* genes can determine protein expression levels (42, 77, 78). Therefore, we next considered polymorphic nucleotides in transcription factor bindings sites (TFbs) of the *KIR3DL3* promoter (19). We aligned reads from targeted DNA sequencing of the *KIR* genomic region to the hg38 genome and identified single nucleotide polymorphism using samtools (79). We identified an ETS site in Papua New Guineans that is triallelic (−53G to A/T) and an Oct-B2 site that is triallelic (−130G to T in Papua New Guineans, −134G to T in Europeans). However, particularly striking was a CREB site with a variant (−110G to C) that is absent from some populations but has risen to moderate frequency in others (e.g. 16.5% in KhoeSan from Southern Africa) (Fig. 6K). This site is quadrallelic world-wide, although A and T are rare (<1%). Additionally, the nucleotide directly upstream is polymorphic and has the second greatest frequency (3.2% in South Asia) of the TFbs positions (−111C to T). These variants are unlinked and therefore segregating independently in the human population. In addition, transcription factor binding site prediction using PROMO (80) suggests that while CREB, c-Jun, and ATF transcription factors can bind this region (with −111C and −110G), variants −111T and −110C are expected to remove binding ability.

To test whether these natural variants have functional impact, we cloned the KIR3DL3 proximal promoter upstream of luciferase and introduced the relevant mutations. We transfected 293T cells and measured luciferase as a proxy for promoter activity. The KIR3DL3 proximal promoter induced expression of luciferase. Mutations in the Oct-B2 site (−130T, −134T) did not affect luciferase expression (Fig. 6L). Those (−53A, −53T) in the ETS site only modestly reduced expression. Remarkably, those in the CREB site (−110T, −110C, −111T) completely ablated proximal promoter activity ($p < 0.001$). To rule out off-target mutations from the PCR-based mutagenesis procedure, we independently cloned a proximal promoter from a South Asian individual homozygous for −110C and observed a similar effect (Fig. S10). We also repeated experiments in 721.221 cells to rule out cell type-specific effects (Fig. S10). We conclude that −110 (C=rs111269305) has unique population genetic patterns and segregates multiple mutations with potential to remove proximal promoter activity. These results raise the possibility of differential KIR3DL3 expression across individuals.

Discussion

We show that KIR3DL3 is expressed primarily by CD8+ T and γδ T cells of PBMC, thymus, lung, and multiple regions of the digestive tract. KIR3DL3 expression was also

observed previously in multiple skin samples (Fig. 1A) as well as decidual lymphocytes (27). Accordingly, we identified that KIR3DL3 expression is upregulated alongside or downstream from TCR stimulation, and this expression can inhibit TCR-mediated stimulation upon binding the HHLA2 ligand. Inhibition may raise the activation threshold, allowing stronger immune responses upon ligand downregulation, akin to missing-self responses mediated by other inhibitory KIR. Contrasting other KIR, which primarily are MHC class I receptors expressed by NK cells, KIR3DL3 bears striking similarities with murine Ly49E. Ly49E recognizes a non-MHC molecule as a ligand (81), is induced downstream of TCR stimulation in peripheral blood (82), and is expressed in intestinal intra-epithelial γδ T cells (82, 83), epidermal γδ T cells, and fetal NK cells (84–86). These similarities suggest that, in addition to detecting loss of MHC class I expression and mediating early placentation, the vital, evolutionary conserved functions of KIR and Ly49 (87) (88) include inhibition of tissue resident cells to maintain homeostasis.

Intraepithelial lymphocytes are comprised of T cells that express αβ or γδ rearranged TCRs, their functions include maintaining epithelial integrity and responding rapidly to infections (89, 90). That KIR3DL3 can be expressed by over 50% of γδ IELs suggests an important biological role for this inhibitory receptor in the digestive tract. Indeed, CD28H, an activating receptor that also recognizes HHLA2, is expressed by IELs (91), and HHLA2 is most highly expressed in the small intestine epithelium (44). As such, interplay with KIR3DL3-HHLA2 likely balances the CD28H-HHLA2 stimulatory signal. KIR3DL3+ T cells in peripheral blood share many attributes with unconventional IELs, which have been described previously as having a “resting-but-activated” phenotype (92). Innate-like CD8αα+ intraepithelial T cells are enriched for auto-reactive T cells, can be hyporesponsive to TCR engagement, rearrange TCR-α chains early in agonistic thymic selection, or are Vδ1-biased, and upregulate NK cell inhibitory receptors and TCR-responsive genes (90, 92–94). The transcriptional profile, cell surface receptor phenotype ($CD3^{low}CD27^{hi}$CCR7-CD69+CD56+), and TCR repertoire of KIR3DL3-expressing T cells reflect these features. KIR3DL3+ cells can be hypofunctional (i.e. proliferate poorly and have reduced CD25 upregulation), with a compromised metabolic signature, and upregulate certain genes canonically downstream of TCR stimulation, consistent with a model of anergy induced by chronic TCR stimulation or agonistic selection (95–97). Additionally, KIR3DL3 is preferentially upregulated in Vδ1+ γδ T cells or CD8+ αβ T cells with early rearranging TCR-α chains, both of which can have autoreactive properties (58, 98–100). These patterns are consistent with an unconventional mode of T cell activation associated with KIR3DL3 expression. The similarity between KIR3DL3+ peripheral T cells and IEL populations may suggest a common thymic developmental origin or the eventual recruitment of circulating KIR3DL3+ cells to HHLA2+ tissues, such as the lungs or digestive tract. Alternatively, peripheral KIR3DL3 expression could be upregulated during the early differentiation of “induced” conventional IELs (90, 92).

The limitations of this study include that the role for KIR3DL3 protein polymorphism remains unsolved, as does the role of KIR3DL3 in reproduction or disease. Although KIR3DL3 is highly polymorphic (19), we observed no strong differences in HHLA2 binding or effector responses across the variable residues. Because the diversity of KIR3DL3 has been shaped by natural selection (19), we anticipate any function of the protein

polymorphism to be revealed through examination of disease cohorts. Contrasting the majority of amino acid variations, we identified that multiple polymorphic nucleotides in the proximal KIR3DL3 promoter can ablate expression of this inhibitory receptor. In a model where KIR3DL3 is induced as an immune checkpoint, this ablation could bias CD28H+ lymphocytes toward continued activation. Recently, a population of KIR+CD8+ regulatory T cells was identified at elevated levels in patients with autoimmune diseases (101). This population has been likened to Ly49+CD8+ T cells which are capable of suppressing pathogenic CD4+ T cells in a murine model of systemic lupus erythematosus-like disease (102). We propose parallels exist between KIR3DL3+ T cells and the regulatory CD8+ T cell populations described. For example, Ly49 expression was induced following canonical antigenic stimulation and was observed to gradually accumulate on self-reactive T cells (103). In addition, Ly49+ regulatory CD8+ T cells express CD44 and CD122 (102), and we observed higher expression of CD122 (IL2RB) in KIR3DL3+ T cells. A greater proportion of KIR3DL3+ T cells express FCRL3 as compared to other T cell subsets. FCRL3 marks a Treg population specified in the thymus that are hyporesponsive to antigenic stimulation (104). These similarities support our hypothesis that KIR3DL3 marks a self-reactive and hyporesponsive T cell subset. Determination of the regulatory properties of KIR3DL3+ T cells will be a necessary step in selecting appropriate therapeutic modalities to target KIR3DL3 in autoimmune disease and cancer.

In the context of tumor immunity, widespread upregulation of HHLA2 has implicated KIR3DL3 as a potential target for immune checkpoint blockade (22, 32–35), especially for tumors that upregulate HHLA2 and resist current treatment targeting checkpoint inhibitors. Our results suggest that cancers of the digestive tract and lung may be the most promising clinical indications to pursue, and indeed we observed KIR3DL3 expression in non-small cell lung cancer, gastric carcinoma, rectal adenocarcinoma, and colorectal tumor, alongside other diverse cancers. Additionally, we confirmed KIR3DL3 expression at the protein level in tissue-resident TILs in metastatic melanoma. The observation of −110C homozygotes may further suggest minimal undesirable off-tumor on-target effects, assuming these individuals remain healthy with naturally low KIR3DL3 cell surface expression.

Together, our data suggest a conserved and essential function for KIR3DL3 in activated and innate-like T cells at mucosal sites such as the lung and intestine. Our work lays the foundation for future studies on the significance of KIR3DL3, and its polymorphic residues, in immune-mediated disease, and further informs the utility of KIR3DL3-HHLA2 interaction as an immunotherapeutic target.

Materials and Methods

Study design—The goal of this study was to characterize the tissue distribution, immunological significance, and natural variation of KIR3DL3 expression by human lymphocytes. Lymphocytes from peripheral blood, lungs, thymus and gastrointestinal tract were assessed by multi-dimensional spectral flow cytometry. As we observed KIR3DL3 is mainly expressed by T cells, we determined phenotypic and transcriptomic profiles of KIR3DL3+ T cells isolated from peripheral blood using scRNAseq, with confirmation by flow cytometry. T cell regulating function was investigated using cell lines engineered

in vitro to express KIR3DL3. The impact of KIR3DL3 polymorphism on cell surface expression, ligand binding and effector activity was examined by cloning specific variants into suitable cell lines in vitro. The number of biological and technical replicates, and statistical tests are listed in the figure legends.

Human Tissues—Healthy donor de-identified peripheral blood was obtained for the Human Immune Tissue Network Biobank by the University of Colorado Clinical and Translation Research Center (CTRC), in sodium heparin tubes. PBMC were isolated using Ficoll gradient (Cytiva). In addition, plateletpheresis leukoreduction filter (LRS chambers) were purchased from Vitalant Blood Center (Denver, CO, USA). Thymus tissues were obtained and processed within 1 hour after extraction from infants undergoing corrective surgeries for congenital heart disease. De-identified human lungs were procured from deceased organ donors by either Donor Alliance (Denver, CO, USA) or the International Institute for the Advancement of Medicine (Edison, NJ, USA). Donors were non-smokers who had no history of lung disease, including no emphysema or other smoking-related lung disease, and who died of non-pulmonary causes. All donors were ventilated endotracheally for three days or less prior to organ donation. Lung tissues were processed immediately upon arrival and always within 24 hours of death. The main pulmonary artery was perfused with phosphate buffered saline (PBS) until the venous output was clear. Subjects had no history of lung disease, including no emphysema or other smoking-related lung disease. Melanoma tissues were collected at the University of Colorado, International Melanoma Biorepository. Healthy sections of jejunum, duodenum, and colon tissues were obtained from organ donors and patients undergoing surgical resections. Ethical approval was granted by the Colorado Multiple Institutional Review Board (COMIRB) protocol #21–4748. Ethical approval for melanoma metastases was granted by the COMIRB protocol #05–0309. PBMC were collected under COMIRB #17–2159. All patients provided written informed consent. The donor metadata are summarized in Table S3.

For thymus, tissue was placed in complete RPMI 1640 media (Gibco, #22400–071), with 10% heat-inactivated fetal bovine serum (FBS, Sigma-Aldrich), 1% non-essential amino acids (Sigma-Aldrich), 1% Sodium Pyruvate (Sigma-Aldrich), 1X GlutaMAX (Gibco), 1% Penicillin/Streptomycin (Gibco), and 1X 2-mercaptoethanol (BME, Sigma-Aldrich)), cut into small pieces, and gently pressed with the back of a 10 ml syringe to release thymocytes. Thymocytes were then isolated by Ficoll gradient. Lung tissues (10–25 grams/donor) were minced to a liquid consistency, prior to dilution with digestion mix (4.0 mg/mL Collagenase D and 0.6 mg/mL DNAse I (both Sigma-Aldrich), diluted in RPMI), then transferred to gentleMACS C tubes. Lymphocytes were dissociated using gentleMACS program m_lung_01_02 five times followed by m_liver_03_01 once, incubated while shaking at 37°C for 1 hour, then one round of the m_liver_04_01 program. Tissue debris was filtered using a metal cell strainer and red blood cells were lysed with ACK lysis buffer. Jejunum, duodenum, and colon samples were minced into IEL dissociation buffer (PBS, 10 mM DTT, 5 mM EDTA, 10 mM HEPES, 5% FBS) and incubated at 37°C while shaking for 30 min. IEL dissociation buffer was replaced once and this process repeated. Debris was filtered and red blood cells lysed with ACK lysis buffer. Lymphocytes from all sources were

washed twice in complete media before cell surface staining or cryopreservation in FBS and 10% DMSO.

Identification of KIR3DL3 reads in Short Read Archive samples—To identify RNA sequencing datasets containing KIR3DL3 transcripts, the first 1,000,000 fastq reads were downloaded from each of the human transcriptomic studies with PolyA selection that were publicly available in the Short Read Archive (SRA). For each downloaded sample (N=360,787), the raw sequencing text data was searched for CTTGCAGGGACCTACAGATGCTTTGGTTCTGTCACTCACTTACCCTATGAGTTGTC, corresponding to position 565–620 in the KIR3DL3 CDS. This sequence is conserved across KIR3DL3 alleles and unique to human KIR3DL3. Traditional mapping methods for the highly polymorphic and homologous *KIR* genomic region would be unable to map reads of KIR3DL3 from RNA transcripts. KIR3DL3+ SRA records were combined according to donor ID, and those that were *ex vivo* or *in vitro* experiments were removed. Notably, while this approach is highly specific in identifying KIR3DL3 expression, requirement of an exact search string to be present in the raw data reduces sensitivity, especially for samples having low KIR3DL3 expression.

Determination of KIR3DL3 antibody specificity—We tested the binding properties of three anti-KIR3DL3 antibody clones: 1136B (R&D), 26E10 (23), and CH21 (27). 1136B could appropriately identify cell lines transduced with KIR3DL3, but exclusively recognized pre-apoptotic cells in PBMCs, as evidenced by colocalization of Annexin V and 1136B (Fig. S1A), suggesting this clone is not appropriate for *ex vivo* staining. CH21 staining of PBMC (Fig. S1B–C) and transduced cell lines (Fig. S1D–E), and KIR expression in scRNA-seq data from sorted blood NK cells (Fig. S1G), show CH21 is a monoclonal antibody specific for KIR3DL3, as previously reported (27). By contrast, staining of PBMC (Fig. S1B–C) and KIR-transduced cell lines (Fig. S1D–E) with 26E10 showed this antibody reacts with both KIR3DL1 and KIR3DL3. Re-analysis of published transcriptome data on sorted 26E10+ PBMCs (23) supports this conclusion (Fig. S1F). Analysis of KIR gene expression in our scRNA-seq data was assessed using BLAST to assign reads to *KIR* genes and alleles, keeping only reads unique to a given *KIR* gene (Fig. S1G).

Single cell RNA sequencing library preparation—Single cell whole transcriptomes and TCR sequencing libraries were prepared using the BD Rhapsody Single-Cell Analysis System (BD Biosciences) according to the manufacturer's specifications. From 5 PBMC donors, 4 populations were sorted after viability, doublet, B cell (CD19+) and monocyte (CD14+) discrimination: 1. NK cells (CD3-CD56+), 2. CD8+ T cells (CD3+CD8+), 3. γδ T cells (CD3+TCRγδ +), and 4. Enriched KIR3DL3+ (CH21+) cells. Cell subsets for the populations from different donors were labelled simultaneously with the cell surface sorting panel (Table S4) an oligonucleotide-tagged antibody sample tag (BD Biosciences) prior to cell sorting on a FACSAria3 (BD Biosciences) (Fig. S11). Prior to cDNA library preparation for the WTA and VDJ libraries, all cell subsets from each donor were pooled, with up to 12 unique sample tags combined per library. Libraries were sequenced using an Illumina NovaSeq.

scRNA sequencing analysis—Quality control, demultiplexing, and read mapping were performed using the BD Rhapsody WTA Analysis Pipeline (v1.0) on the Seven Bridges server. Count and meta data were loaded into Seurat (v4.1.0) for quality filtering of cells based on mitochondrial contamination (<25% of UMI counts) and sequencing breadth (200–4000 expressed genes per cell) (47). Normalization, clustering, dimension reduction, and multimodal reference mapping were also performed in Seurat. For the latter, the dataset was mapped to a CITE-seq reference dataset (47), transferring over the population labels to the cells. Based on these labels, contaminating CD4+ T and B cells were removed from the dataset. Analyses was focused on NK, CD8+ T, and γδ T cell subsets. Differential gene expression was performed comparing KIR3DL3+ and KIR3DL3- cells of the following subsets: naïve CD8+, central memory CD8+, effector memory CD8+, and γδ T cells. The top 10 genes from each of these comparisons are presented in Fig. 4D. VISION (v3.0.0) was used to calculate a Naïve Score and a TCR Activation Score, which is the sum of normalized expression values of a chosen gene set. Genes for the naïve score were those genes that specifically defined ($p<0.001$) naïve CD8+ T cells in our data. Genes for the TCR activation score were established immediate-early or early TCR-responsive genes with prior evidence of RNA upregulation following TCR stimulation. The fgsea R package (v.1.20.0) was used for gene enrichment analyses (53). For VDJ TCR repertoire analyses, frequencies of shared TRAV, TRBV, TRGV, and TRDV genes across the five donors were compared for KIR3DL3+ and KIR3DL3- cells. A mixed effects model in MCMCglmm was used with a fixed effect associated with KIR3DL3 expression and random effects associated with donor, V gene, and the interaction of V genes with KIR3DL3. The latter random effect was used to determine if V gene usage was significantly altered in KIR3DL3+ cells. All data and code required to replicate analyses are available on figshare (https://doi.org/10.6084/m9.figshare.c.6651410.v2).

T cell receptor stimulation—One million cells PBMCs were incubated in 24 well plates containing 30 IU/mL IL-2 (NCI), with or without Human T-Activator CD3/CD28 dynabeads (ThermoFisher). To ensure all T cells were stimulated, 25 μL of dynabeads were used per well. After 48 hours, beads were removed by magnetic separation. At 7 days, cells were stained with viability dye-efluor506, CH21, anti-Ms IgG PE, and fluorescent-conjugated antibodies; anti-CD3, CD56, CD14, CD19, TCRγδ, Vδ1, and Vδ2 (Table S4). Samples were acquired on the Cytek Aurora to determine the proportion of KIR3DL3+ cells and total T cells. Fold expansion of either all T cells or KIR3DL3+ T cells was calculated as relative to unstimulated T cells.

Calcium mobilization assay—IIa1.6-KIR3DL3 cells were created as described in Supplementary Materials and Methods, with exception that the Phoenix-Eco packaging line and pMXs-KIR3DL3*001 (27) were used. IIa1.6-KIR3DL3 cells were loaded with 2 μM Indo-1AM calcium sensing dye (eBioscience) and stained with either 0.5 μg/mL or 0.2 μg/mL biotinylated Fab anti-IgG (Jackson Laboratories) and 20ug/mL of biotinylated anti-KIR3DL3 (clone CH21) and coaggregated with 20ug/mL Avidin (Sigma). Relative intracellular free calcium was measured over time using flow cytometry with a BD LSR Fortessa X-20 instrument. Intracellular Ca^{2+} was analyzed as the 405 nm/485 nm ratio using FlowJo software (v10.8.1). Area under the curve was corrected to the baseline calcium

mobilization value for each sample and peak flux value was calculated with baseline subtraction. 20 μg/mL of biotinylated CD22 (clone CY34) was used as a positive control (105).

Jurkat-9C2-KIR3DL3 cells (67) were created using pMXs-KIR3DL3*003. Calcium mobilization was performed as described in the IIa1.6 model, with exception that prior to avidin crosslinking, Jurkat-9C2-KIR3DL3 cells were incubated with 5 μg/mL biotinylated anti-CD3 (clone OKT3; Biolegend) with or without 25ug/mL of biotinylated anti-KIR3DL3 (clone CH21). Area under the curve was corrected to the baseline calcium mobilization value for each sample and peak flux value was calculated with baseline subtraction.

NFAT luciferase assay—Jurkat-NFAT-Luc cells (68) (Jurkat-NFAT-Luc) were transduced to express KIR3DL3, using pMXs-KIR3DL3*003. CHO-αCD3 cells (68) (CHO-αCD3) were transduced to express HHLA2, using the pMXs-IRES-puro retroviral expression vector (CellBio Labs). CHO-αCD3 or CHO-αCD3-HHLA2 cells were seeded at 2×10^4/well density in CHO-K1 growth medium in a white flat bottom 96 well plate (Thermo Scientific 165306) and incubated overnight at 37°C with 5% CO_2. The medium was then removed, and cells were incubated with 2.5μg/mL KIR3DL3 blocking antibody 26E10 (23), or no antibody, in 50μL Jurkat cell media for one hour before the addition of Jurkat-NFAT-Luc or Jurkat-NFAT-Luc-KIR3DL3 cells at 1×10^5/well in 50μL Jurkat cell media. After 4hrs, cells were lysed using the One-Glo system (Promega), and luminescence was immediately analyzed using a luminescence plate reader (Tecan Infinite M Plex).

HHLA2-Fc binding assay—NKL cells (1×10^5) were washed with PBS, stained with Fixable Viability Dye eFluor 780 (eBioScience; 1:20000), washed with FACS buffer (PBS, 0.5% BSA, 0.1% NaN_3), then incubated with an HHLA2-Fc fusion protein (Q9UM44; R&D) at 100 μg/mL in PBS for 30 minutes. Cells were then stained with labelled anti-KIR3DL3-PE (clone 1136B; R&D) and anti-HHLA2-APC (clone MA57YW; eBioscience) and fluorescent intensity measured using a Cytek Northern Lights instrument.

Luciferase assays for promoter activity—The KIR3DL3 proximal promoter (271 bp upstream of the first codon) was amplified from a single individual (73), using primers (Table S5) that introduced a 5’ KpnI site and a 3’ XhoI site, and cloned into the pGL3 firefly luciferase vector (Promega). Site directed mutagenesis was performed as described (Supplementary Materials and Methods), with overlapping primers introducing each mutation of interest (Table S5). 1×10^5 721.221 or 293T cells were plated in 24 well plates and transfected with 400 ng of pGL3 and 100 ng of pRL-CMV (Promega). Two days later, cells were lysed, and luciferase activity measured using the Dual Luciferase Kit (Promega). Significance was assessed using a linear model (lm function in R).

Population genetic analysis of the KIR3DL3 promoter—Sequence reads specific to the *KIR* genomic region were obtained from multiple studies as described (8, 19, 106). The sequence reads were aligned to GRCh38 using bwa (v0.7.17) (107) and promoter variants (within 500bp upstream of the KIR3DL3 ATG start codon) called using samtools mpileup (v1.7) (79).

Statistical analyses

All statistics were performed using generalized linear mixed models fit in MCMCglmm (108) (v2.33), with R code and raw data available on figshare (https://doi.org/10.6084/m9.figshare.c.6651410.v2). Significance for a specific parameter was assessed by the proportion of MCMC iterations that overlap zero (two-tailed, alpha = 0.05). 95% highest posterior density intervals were reported as confidence intervals. Differentially expressed genes from single cell data were determined by a Wilcoxon rank sum test and corrected with the Bonferroni method, as implemented in Seurat.

Supplementary Material

Refer to Web version on PubMed Central for supplementary material.

Acknowledgments:

We are grateful to Ashley Moffett for providing CH21, and Xingxing Zang for providing 26E10 monoclonal antibody. The 9C2 Jurkat cells were a kind gift from Adam Uldrich. We acknowledge the BRB Preclinical Biologics Repository for provision of IL-2, the University of Colorado, Anschutz Medical Campus ImmunoMicro Flow Cytometry Shared Resource (RRID:SCR_021321), Barbara Davis Center Flow Cytometry Services and the AMC Genomics and Microarray Core. We acknowledge the University of Colorado, AMC Pathology Shared Resource and and IBD Biobank #14-2012 for coordinating donor tissue samples. We would also like to thank William A Robinson and Kasey L Couts from the University of Colorado International Melanoma Biorepository.

Funding:

This work was supported by the following funding sources: National Institutes of Health NIAID 1R56AI155729-01 (PN). ACS IRG #16–184-56 from the American Cancer Society to the University of Colorado Cancer Center (LL). NIH Fellowship F32 AI161790 (WP). NIH T32 AI07405 (LAL). JT was funded by the European Research Council (ERC) under the European Union's Horizon 2020 research and innovation programme (grant no. 695551). NIH grants R35HL140039, R01HL130938, and R01HL149741 (WJ). JR was supported by an NHMRC Australia Investigator award. PBMC collection was supported by NIH/NCATS Colorado CTSA Grant Number UL1 TR002535.

Data and materials availability:

Original RNA sequencing data have been deposited to GEO: GSE232917. All data needed to evaluate the conclusions in the paper are present in the paper or the Supplementary Materials, and at https://doi.org/10.6084/m9.figshare.c.6651410.v2 alongside any bespoke code used for analysis. Cell lines and other materials are available upon request.

References

1. Ali A, Gyurova IE, Waggoner SN, Mutually assured destruction: the cold war between viruses and natural killer cells. Current opinion in virology 34, 130–139 (2019). [PubMed: 30877885]
2. Hammer Q, Ruckert T, Romagnani C, Natural killer cell specificity for viral infections. Nature immunology 19, 800–808 (2018). [PubMed: 30026479]
3. Jost S, Altfeld M, Control of human viral infections by natural killer cells. Annual review of immunology 31, 163–194 (2013).
4. Locatelli F, Pende D, Falco M, Della Chiesa M, Moretta A, Moretta L, NK Cells Mediate a Crucial Graft-versus-Leukemia Effect in Haploidentical-HSCT to Cure High-Risk Acute Leukemia. Trends Immunol 39, 577–590 (2018). [PubMed: 29793748]
5. Parham P, Moffett A, Variable NK cell receptors and their MHC class I ligands in immunity, reproduction and human evolution. Nature reviews. Immunology 13, 133–144 (2013).

6. Venstrom JM, Pittari G, Gooley TA, Chewning JH, Spellman S, Haagenson M, Gallagher MM, Malkki M, Petersdorf E, Dupont B, Hsu KC, HLA-C-dependent prevention of leukemia relapse by donor activating KIR2DS1. The New England journal of medicine 367, 805–816 (2012). [PubMed: 22931314]
7. Vivier E, Raulet DH, Moretta A, Caligiuri MA, Zitvogel L, Lanier LL, Yokoyama WM, Ugolini S, Innate or adaptive immunity? The example of natural killer cells. Science 331, 44–49 (2011). [PubMed: 21212348]
8. Pollock NR, Harrison GF, Norman PJ, Immunogenomics of Killer Cell Immunoglobulin-Like Receptor (KIR) and HLA Class I: Coevolution and Consequences for Human Health. J Allergy Clin Immunol Pract 10, 1763–1775 (2022). [PubMed: 35561968]
9. Long EO, Kim HS, Liu D, Peterson ME, Rajagopalan S, Controlling natural killer cell responses: integration of signals for activation and inhibition. Annual review of immunology 31, 227–258 (2013).
10. Anfossi N, Andre P, Guia S, Falk CS, Roetynck S, Stewart CA, Breso V, Frassati C, Reviron D, Middleton D, Romagne F, Ugolini S, Vivier E, Human NK cell education by inhibitory receptors for MHC class I. Immunity 25, 331–342 (2006). [PubMed: 16901727]
11. Bjorkstrom NK, Beziat V, Cichocki F, Liu LL, Levine J, Larsson S, Koup RA, Anderson SK, Ljunggren HG, Malmberg KJ, CD8 T cells express randomly selected KIRs with distinct specificities compared with NK cells. Blood 120, 3455–3465 (2012). [PubMed: 22968455]
12. Boelen L, Debebe B, Silveira M, Salam A, Makinde J, Roberts CH, Wang ECY, Frater J, Gilmour J, Twigger K, Ladell K, Miners KL, Jayaraman J, Traherne JA, Price DA, Qi Y, Martin MP, Macallan DC, Thio CL, Astemborski J, Kirk G, Donfield SM, Buchbinder S, Khakoo SI, Goedert JJ, Trowsdale J, Carrington M, Kollnberger S, Asquith B, Inhibitory killer cell immunoglobulin-like receptors strengthen CD8(+) T cell-mediated control of HIV-1, HCV, and HTLV-1. Sci Immunol 3, eaao2892 (2018). [PubMed: 30413420]
13. Young NT, Uhrberg M, Phillips JH, Lanier LL, Parham P, Differential expression of leukocyte receptor complex-encoded Ig-like receptors correlates with the transition from effector to memory CTL. J Immunol 166, 3933–3941 (2001). [PubMed: 11238638]
14. Alter G, Rihn S, Streeck H, Teigen N, Piechocka-Trocha A, Moss K, Cohen K, Meier A, Pereyra F, Walker B, Altfeld M, Ligand-independent exhaustion of killer immunoglobulin-like receptor-positive CD8+ T cells in human immunodeficiency virus type 1 infection. J Virol 82, 9668–9677 (2008). [PubMed: 18579582]
15. Ugolini S, Arpin C, Anfossi N, Walzer T, Cambiaggi A, Förster R, Lipp M, Toes RE, Melief CJ, Marvel J, Vivier E, Involvement of inhibitory NKRs in the survival of a subset of memory-phenotype CD8+ T cells. Nature immunology 2, 430–435 (2001). [PubMed: 11323697]
16. Uhrberg M, Valiante NM, Shum BP, Shilling HG, Lienert-Weidenbach K, Corliss B, Tyan D, Lanier LL, Parham P, Human diversity in killer cell inhibitory receptor genes. Immunity 7, 753–763 (1997). [PubMed: 9430221]
17. Wilson MJ, Torkar M, Haude A, Milne S, Jones T, Sheer D, Beck S, Trowsdale J, Plasticity in the organization and sequences of human KIR/ILT gene families. Proc Natl Acad Sci U S A 97, 4778–4783. (2000). [PubMed: 10781084]
18. Hsu KC, Chida S, Geraghty DE, Dupont B, The killer cell immunoglobulin-like receptor (KIR) genomic region: gene-order, haplotypes and allelic polymorphism. Immunological reviews 190, 40–52 (2002). [PubMed: 12493005]
19. Leaton LA, Shortt J, Kichula KM, Tao S, Nemat-Gorgani N, Mentzer AJ, Oppenheimer SJ, Deng Z, Hollenbach JA, Gignoux CR, Guethlein LA, Parham P, Carrington M, Norman PJ, Conservation, Extensive Heterozygosity, and Convergence of Signaling Potential All Indicate a Critical Role for KIR3DL3 in Higher Primates. Front Immunol 10, 24 (2019). [PubMed: 30745901]
20. Wojtowicz WM, Vielmetter J, Fernandes RA, Siepe DH, Eastman CL, Chisholm GB, Cox S, Klock H, Anderson PW, Rue SM, Miller JJ, Glaser SM, Bragstad ML, Vance J, Lam AW, Lesley SA, Zinn K, Garcia KC, A Human IgSF Cell-Surface Interactome Reveals a Complex Network of Protein-Protein Interactions. Cell 182, 1027–1043 e1017 (2020). [PubMed: 32822567]
21. Verschueren E, Husain B, Yuen K, Sun Y, Paduchuri S, Senbabaoglu Y, Lehoux I, Arena TA, Wilson B, Lianoglou S, Bakalarski C, Franke Y, Chan P, Wong AW, Gonzalez LC, Mariathasan

S, Turley SJ, Lill JR, Martinez-Martin N, The Immunoglobulin Superfamily Receptome Defines Cancer-Relevant Networks Associated with Clinical Outcome. Cell 182, 329–344 e319 (2020). [PubMed: 32589946]

22. Bhatt RS, Berjis A, Konge JC, Mahoney KM, Klee AN, Freeman SS, Chen CH, Jegede OA, Catalano PJ, Pignon JC, Sticco-Ivins M, Zhu B, Hua P, Soden J, Zhu J, McDermott DF, Arulanandam AR, Signoretti S, Freeman GJ, KIR3DL3 Is an Inhibitory Receptor for HHLA2 that Mediates an Alternative Immunoinhibitory Pathway to PD1. Cancer Immunol Res 9, 156–169 (2021). [PubMed: 33229411]
23. Wei Y, Ren X, Galbo PM, Moerdler S, Wang H, Sica RA, Etemad-Gilbertson B, Shi L, Zhu L, Tang X, Lin Q, Peng M, Guan F, Zheng D, Chinai JM, Zang X, KIR3DL3-HHLA2 is a human immunosuppressive pathway and a therapeutic target. Sci Immunol 6, eabf9792 (2021). [PubMed: 34244312]
24. Freud AG, Mundy-Bosse BL, Yu J, Caligiuri MA, The Broad Spectrum of Human Natural Killer Cell Diversity. Immunity 47, 820–833 (2017). [PubMed: 29166586]
25. Horowitz A, Strauss-Albee DM, Leipold M, Kubo J, Nemat-Gorgani N, Dogan OC, Dekker CL, Mackey S, Maecker H, Swan GE, Davis MM, Norman PJ, Guethlein LA, Desai M, Parham P, Blish CA, Genetic and environmental determinants of human NK cell diversity revealed by mass cytometry. Science translational medicine 5, 208ra145 (2013).
26. Cooley S, Xiao F, Pitt M, Gleason M, McCullar V, Bergemann TL, McQueen KL, Guethlein LA, Parham P, Miller JS, A subpopulation of human peripheral blood NK cells that lacks inhibitory receptors for self-MHC is developmentally immature. Blood 110, 578–586 (2007). [PubMed: 17392508]
27. Trundley AE, Hiby SE, Chang C, Sharkey AM, Santourlidis S, Uhrberg M, Trowsdale J, Moffett A, Molecular characterization of KIR3DL3. Immunogenetics 57, 904–916 (2006). [PubMed: 16391939]
28. Li H, Wright PW, McCullen M, Anderson SK, Characterization of KIR intermediate promoters reveals four promoter types associated with distinct expression patterns of KIR subtypes. Genes and immunity 17, 66–74 (2016). [PubMed: 26656451]
29. van Bergen J, Stewart CA, van den Elsen PJ, Trowsdale J, Stuctural and functional differences between the promoters of independently expressed killer cell Ig-like receptors. European Journal of Immunology 35, 2191–2199 (2005). [PubMed: 15940669]
30. Ohaegbulam KC, Assal A, Lazar-Molnar E, Yao Y, Zang X, Human cancer immunotherapy with antibodies to the PD-1 and PD-L1 pathway. Trends in Molecular Medicine 21, 24–33 (2015). [PubMed: 25440090]
31. Egen JG, Kuhns MS, Allison JP, CTLA-4: new insights into its biological function and use in tumor immunotherapy. Nature immunology 3, 611–618 (2002). [PubMed: 12087419]
32. Chen L, Zhu D, Feng J, Zhou Y, Wang Q, Feng H, Zhang J, Jiang J, Overexpression of HHLA2 in human clear cell renal cell carcinoma is significantly associated with poor survival of the patients. Cancer cell international 19, 101–101 (2019). [PubMed: 31015801]
33. Cheng H, Janakiram M, Borczuk A, Lin J, Qiu W, Liu H, Chinai JM, Halmos B, Perez-Soler R, Zang X, HHLA2, a new immune checkpoint member of the B7 family, is widely expressed in human lung cancer and associated with EGFR mutational status. Clinical Cancer Research 23, 825–832 (2017). [PubMed: 27553831]
34. Jing CY, Fu YP, Yi Y, Zhang MX, Zheng SS, Huang JL, Gan W, Xu X, Lin JJ, Zhang J, Qiu SJ, Zhang BH, HHLA2 in intrahepatic cholangiocarcinoma: An immune checkpoint with prognostic significance and wider expression compared with PD-L1. Journal for ImmunoTherapy of Cancer 7, (2019).
35. Zhu Z, Dong W, Overexpression of HHLA2, a member of the B7 family, is associated with worse survival in human colorectal carcinoma. OncoTargets and Therapy 11, 1563–1570 (2018). [PubMed: 29593422]
36. Frazier WR, Steiner N, Hou L, Dakshanamurthy S, Hurley CK, Allelic Variation in KIR2DL3 Generates a KIR2DL2-like Receptor with Increased Binding to its HLA-C Ligand. The Journal of Immunology 190, 6198–6208 (2013). [PubMed: 23686481]

37. Vivian JP, Duncan RC, Berry R, O'Connor GM, Reid HH, Beddoe T, Gras S, Saunders PM, Olshina MA, Widjaja JM, Harpur CM, Lin J, Maloveste SM, Price DA, Lafont BA, McVicar DW, Clements CS, Brooks AG, Rossjohn J, Killer cell immunoglobulin-like receptor 3DL1-mediated recognition of human leukocyte antigen B. Nature 479, 401–405 (2011). [PubMed: 22020283]
38. Winter CC, Long EO, A single amino acid in the p58 killer cell inhibitory receptor controls the ability of natural killer cells to discriminate between the two groups of HLA-C allotypes. Journal of immunology (Baltimore, Md. : 1950) 158, 4026–4028 (1997). [PubMed: 9126959]
39. Yawata M, Yawata N, Draghi M, Little AM, Partheniou F, Parham P, Roles for HLA and KIR polymorphisms in natural killer cell repertoire selection and modulation of effector function. Journal of Experimental Medicine 203, 633–645 (2006). [PubMed: 16533882]
40. Nemat-Gorgani N, Hilton HG, Henn BM, Lin M, Gignoux CR, Myrick JW, Werely CJ, Granka JM, Moller M, Hoal EG, Yawata M, Yawata N, Boelen L, Asquith B, Parham P, Norman PJ, Different Selected Mechanisms Attenuated the Inhibitory Interaction of KIR2DL1 with C2(+) HLA-C in Two Indigenous Human Populations in Southern Africa. J Immunol 200, 2640–2655 (2018). [PubMed: 29549179]
41. Bari R, Bell T, Leung WH, Vong QP, Chan WK, Das Gupta N, Holladay M, Rooney B, Leung W, Significant functional heterogeneity among KIR2DL1 alleles and a pivotal role of arginine 245. Blood 114, 5182–5190 (2009). [PubMed: 19828694]
42. Vilches C, Gardiner CM, Parham P, Gene structure and promoter variation of expressed and nonexpressed variants of the KIR2DL5 gene. J Immunol 165, 6416–6421 (2000). [PubMed: 11086080]
43. Wright PW, Li H, Huehn A, O'Connor GM, Cooley S, Miller JS, Anderson SK, Characterization of a weakly expressed KIR2DL1 variant reveals a novel upstream promoter that controls KIR expression. Genes and immunity 15, 440–448 (2014). [PubMed: 24989671]
44. Wang D, Eraslan B, Wieland T, Hallström B, Hopf T, Zolg DP, Zecha J, Asplund A, Li LH, Meng C, Frejno M, Schmidt T, Schnatbaum K, Wilhelm M, Ponten F, Uhlen M, Gagneur J, Hahne H, Kuster B, A deep proteome and transcriptome abundance atlas of 29 healthy human tissues. Mol Syst Biol 15, e8503 (2019). [PubMed: 30777892]
45. Van Acker HH, Capsomidis A, Smits EL, Van Tendeloo VF, CD56 in the Immune System: More Than a Marker for Cytotoxicity? Front Immunol 8, 892 (2017). [PubMed: 28791027]
46. Corgnac S, Malenica I, Mezquita L, Auclin E, Voilin E, Kacher J, Halse H, Grynszpan L, Signolle N, Dayris T, Leclerc M, Droin N, de Montpréville V, Mercier O, Validire P, Scoazec JY, Massard C, Chouaib S, Planchard D, Adam J, Besse B, Mami-Chouaib F, CD103(+)CD8(+) T(RM) Cells Accumulate in Tumors of Anti-PD-1-Responder Lung Cancer Patients and Are Tumor-Reactive Lymphocytes Enriched with Tc17. Cell Rep Med 1, 100127 (2020). [PubMed: 33205076]
47. Hao Y, Hao S, Andersen-Nissen E, Mauck WM 3rd, Zheng S, Butler A, Lee MJ, Wilk AJ, Darby C, Zager M, Hoffman P, Stoeckius M, Papalexi E, Mimitou EP, Jain J, Srivastava A, Stuart T, Fleming LM, Yeung B, Rogers AJ, McElrath JM, Blish CA, Gottardo R, Smibert P, Satija R, Integrated analysis of multimodal single-cell data. Cell 184, 3573–3587 e3529 (2021). [PubMed: 34062119]
48. DeTomaso D, Jones MG, Subramaniam M, Ashuach T, Ye CJ, Yosef N, Functional interpretation of single cell similarity maps. Nat Commun 10, 4376 (2019). [PubMed: 31558714]
49. Gutierrez-Arcelus M, Teslovich N, Mola AR, Polidoro RB, Nathan A, Kim H, Hannes S, Slowikowski K, Watts GFM, Korsunsky I, Brenner MB, Raychaudhuri S, Brennan PJ, Lymphocyte innateness defined by transcriptional states reflects a balance between proliferation and effector functions. Nature Communications 10, 687 (2019).
50. Flynn JK, Gorry PR, Stem memory T cells (TSCM)-their role in cancer and HIV immunotherapies. Clin Transl Immunology 3, e20 (2014). [PubMed: 25505968]
51. Kelly K, Siebenlist U, Immediate-early genes induced by antigen receptor stimulation. Curr Opin Immunol 7, 327–332 (1995). [PubMed: 7546396]
52. Gallagher MP, Conley JM, Vangala P, Garber M, Reboldi A, Berg LJ, Hierarchy of signaling thresholds downstream of the T cell receptor and the Tec kinase ITK. Proc Natl Acad Sci U S A 118, (2021).

53. Korotkevich G, Sukhov V, Budin N, Shpak B, Artyomov MN, Sergushichev A, Fast gene set enrichment analysis. bioRxiv, 060012 (2021).
54. Myers DR, Wheeler B, Roose JP, mTOR and other effector kinase signals that impact T cell function and activity. Immunological reviews 291, 134–153 (2019). [PubMed: 31402496]
55. Vardhana SA, Hwee MA, Berisa M, Wells DK, Yost KE, King B, Smith M, Herrera PS, Chang HY, Satpathy AT, van den Brink MRM, Cross JR, Thompson CB, Impaired mitochondrial oxidative phosphorylation limits the self-renewal of T cells exposed to persistent antigen. Nature immunology 21, 1022–1033 (2020). [PubMed: 32661364]
56. Willcox CR, Davey MS, Willcox BE, Development and Selection of the Human Vgamma9Vdelta2(+) T-Cell Repertoire. Front Immunol 9, 1501 (2018). [PubMed: 30013562]
57. Boudinot P, Mondot S, Jouneau L, Teyton L, Lefranc M-P, Lantz O, Restricting nonclassical MHC genes coevolve with TRAV genes used by innate-like T cells in mammals. Proceedings of the National Academy of Sciences of the United States of America 113, E2983–E2992 (2016). [PubMed: 27170188]
58. Verstichel G, Vermijlen D, Martens L, Goetgeluk G, Brouwer M, Thiault N, Van Caeneghem Y, De Munter S, Weening K, Bonte S, Leclercq G, Taghon T, Kerre T, Saeys Y, Van Dorpe J, Cheroutre H, Vandekerckhove B, The checkpoint for agonist selection precedes conventional selection in human thymus. Sci Immunol 2, eaah4232 (2017). [PubMed: 28783686]
59. Hendricks DW, Fink PJ, Uneven colonization of the lymphoid periphery by T cells that undergo early TCR{alpha} rearrangements. Journal of immunology (Baltimore, Md. : 1950) 182, 4267–4274 (2009). [PubMed: 19299725]
60. Baldwin TA, Sandau MM, Jameson SC, Hogquist KA, The timing of TCR alpha expression critically influences T cell development and selection. J Exp Med 202, 111–121 (2005). [PubMed: 15998791]
61. Park JE, Botting RA, Dominguez Conde C, Popescu DM, Lavaert M, Kunz DJ, Goh I, Stephenson E, Ragazzini R, Tuck E, Wilbrey-Clark A, Roberts K, Kedlian VR, Ferdinand JR, He X, Webb S, Maunder D, Vandamme N, Mahbubani KT, Polanski K, Mamanova L, Bolt L, Crossland D, de Rita F, Fuller A, Filby A, Reynolds G, Dixon D, Saeb-Parsy K, Lisgo S, Henderson D, Vento-Tormo R, Bayraktar OA, Barker RA, Meyer KB, Saeys Y, Bonfanti P, Behjati S, Clatworthy MR, Taghon T, Haniffa M, Teichmann SA, A cell atlas of human thymic development defines T cell repertoire formation. Science 367, (2020).
62. Kisielow J, Tortola L, Weber J, Karjalainen K, Kopf M, Evidence for the divergence of innate and adaptive T-cell precursors before commitment to the αβ and γδ lineages. Blood 118, 6591–6600 (2011). [PubMed: 22021367]
63. Walker LJ, Marrinan E, Muenchhoff M, Ferguson J, Kloverpris H, Cheroutre H, Barnes E, Goulder P, Klenerman P, CD8alphaalpha Expression Marks Terminally Differentiated Human CD8+ T Cells Expanded in Chronic Viral Infection. Front Immunol 4, 223 (2013). [PubMed: 23964274]
64. Purdy AK, Campbell KS, SHP-2 Expression Negatively Regulates NK Cell Function. The Journal of Immunology 183, 7234 (2009). [PubMed: 19915046]
65. Yusa S, Campbell KS, Src homology region 2-containing protein tyrosine phosphatase-2 (SHP-2) can play a direct role in the inhibitory function of killer cell Ig-like receptors in human NK cells. J Immunol 170, 4539–4547 (2003). [PubMed: 12707331]
66. Yusa S, Catina TL, Campbell KS, SHP-1- and phosphotyrosine-independent inhibitory signaling by a killer cell Ig-like receptor cytoplasmic domain in human NK cells. J Immunol 168, 5047–5057 (2002). [PubMed: 11994457]
67. Uldrich AP, Le Nours J, Pellicci DG, Gherardin NA, McPherson KG, Lim RT, Patel O, Beddoe T, Gras S, Rossjohn J, Godfrey DI, CD1d-lipid antigen recognition by the γδ TCR. Nature immunology 14, 1137–1145 (2013). [PubMed: 24076636]
68. Fujiwara Y, Torphy RJ, Sun Y, Miller EN, Ho F, Borcherding N, Wu T, Torres RM, Zhang W, Schulick RD, Zhu Y, The GPR171 pathway suppresses T cell activation and limits antitumor immunity. Nat Commun 12, 5857 (2021). [PubMed: 34615877]
69. Saunders PM, Vivian JP, O'Connor GM, Sullivan LC, Pymm P, Rossjohn J, Brooks AG, A bird's eye view of NK cell receptor interactions with their MHC class I ligands. Immunological reviews 267, 148–166 (2015). [PubMed: 26284476]

70. Campbell KS, Purdy AK, Structure/function of human killer cell immunoglobulin-like receptors: Lessons from polymorphisms, evolution, crystal structures and mutations. Immunology 132, 315–325 (2011). [PubMed: 21214544]

71. Carr WH, Pando MJ, Parham P, KIR3DL1 Polymorphisms That Affect NK Cell Inhibition by HLA-Bw4 Ligand. The Journal of Immunology 175, 5222 (2005). [PubMed: 16210627]

72. Graef T, Moesta AK, Norman PJ, Abi-Rached L, Vago L, Older Aguilar AM, Gleimer M, Hammond JA, Guethlein LA, Bushnell DA, Robinson PJ, Parham P, KIR2DS4 is a product of gene conversion with KIR3DL2 that introduced specificity for HLA-A*11 while diminishing avidity for HLA-C. J Exp Med 206, 2557–2572 (2009). [PubMed: 19858347]

73. Norman PJ, Abi-Rached L, Gendzekhadze K, Korbel D, Gleimer M, Rowley D, Bruno D, Carrington CV, Chandanayingyong D, Chang YH, Crespi C, Saruhan-Direskeneli G, Fraser PA, Hameed K, Kamkamidze G, Koram KA, Layrisse Z, Matamoros N, Mila J, Park MH, Pitchappan RM, Ramdath DD, Shiau MY, Stephens HA, Struik S, Verity DH, Vaughan RW, Tyan D, Davis RW, Riley EM, Ronaghi M, Parham P, Unusual selection on the KIR3DL1/S1 natural killer cell receptor in Africans. Nature genetics 39, 1092–1099 (2007). [PubMed: 17694054]

74. Auton A, Abecasis GR, Altshuler DM, Durbin RM, Bentley DR, Chakravarti A, Clark AG, Donnelly P, Eichler EE, Flicek P, Gabriel SB, Gibbs RA, Green ED, Hurles ME, Knoppers BM, Korbel JO, Lander ES, Lee C, Lehrach H, Mardis ER, Marth GT, McVean GA, Nickerson DA, Schmidt JP, Sherry ST, Wang J, Wilson RK, Boerwinkle E, Doddapaneni H, Han Y, Korchina V, Kovar C, Lee S, Muzny D, Reid JG, Zhu Y, Chang Y, Feng Q, Fang X, Guo X, Jian M, Jiang H, Jin X, Lan T, Li G, Li J, Li Y, Liu S, Liu X, Lu Y, Ma X, Tang M, Wang B, Wang G, Wu H, Wu R, Xu X, Yin Y, Zhang D, Zhang W, Zhao J, Zhao M, Zheng X, Gupta N, Gharani N, Toji LH, Gerry NP, Resch AM, Barker J, Clarke L, Gil L, Hunt SE, Kelman G, Kulesha E, Leinonen R, McLaren WM, Radhakrishnan R, Roa A, Smirnov D, Smith RE, Streeter I, Thormann A, Toneva I, Vaughan B, Zheng-Bradley X, Grocock R, Humphray S, James T, Kingsbury Z, Sudbrak R, Albrecht MW, Amstislavskiy VS, Borodina TA, Lienhard M, Mertes F, Sultan M, Timmermann B, Yaspo ML, Fulton L, Ananiev V, Belaia Z, Beloslyudtsev D, Bouk N, Chen C, Church D, Cohen R, Cook C, Garner J, Hefferon T, Kimelman M, Liu C, Lopez J, Meric P, O'Sullivan C, Ostapchuk Y, Phan L, Ponomarov S, Schneider V, Shekhtman E, Sirotkin K, Slotta D, Zhang H, Balasubramaniam S, Burton J, Danecek P, Keane TM, Kolb-Kokocinski A, McCarthy S, Stalker J, Quail M, Davies CJ, Gollub J, Webster T, Wong B, Zhan Y, Campbell CL, Kong Y, Marcketta A, Yu F, Antunes L, Bainbridge M, Sabo A, Huang Z, Coin LJM, Fang L, Li Q, Li Z, Lin H, Liu B, Luo R, Shao H, Xie Y, Ye C, Yu C, Zhang F, Zheng H, Zhu H, Alkan C, Dal E, Kahveci F, Garrison EP, Kural D, Lee WP, Leong WF, Stromberg M, Ward AN, Wu J, Zhang M, Daly MJ, DePristo MA, Handsaker RE, Banks E, Bhatia G, Del Angel G, Genovese G, Li H, Kashin S, McCarroll SA, Nemesh JC, Poplin RE, Yoon SC, Lihm J, Makarov V, Gottipati S, Keinan A, Rodriguez-Flores JL, Rausch T, Fritz MH, Stütz AM, Beal K, Datta A, Herrero J, Ritchie GRS, Zerbino D, Sabeti PC, Shlyakhter I, Schaffner SF, Vitti J, Cooper DN, Ball EV, Stenson PD, Barnes B, Bauer M, Cheetham RK, Cox A, Eberle M, Kahn S, Murray L, Peden J, Shaw R, Kenny EE, Batzer MA, Konkel MK, Walker JA, MacArthur DG, Lek M, Herwig R, Ding L, Koboldt DC, Larson D, Ye K, Gravel S, Swaroop A, Chew E, Lappalainen T, Erlich Y, Gymrek M, Willems TF, Simpson JT, Shriver MD, Rosenfeld JA, Bustamante CD, Montgomery SB, De La Vega FM, Byrnes JK, Carroll AW, DeGorter MK, Lacroute P, Maples BK, Martin AR, Moreno-Estrada A, Shringarpure SS, Zakharia F, Halperin E, Baran Y, Cerveira E, Hwang J, Malhotra A, Plewczynski D, Radew K, Romanovitch M, Zhang C, Hyland FCL, Craig DW, Christoforides A, Homer N, Izatt T, Kurdoglu AA, Sinari SA, Squire K, Xiao C, Sebat J, Antaki D, Gujral M, Noor A, Ye K, Burchard EG, Hernandez RD, Gignoux CR, Haussler D, Katzman SJ, Kent WJ, Howie B, Ruiz-Linares A, Dermitzakis ET, Devine SE, Kang HM, Kidd JM, Blackwell T, Caron S, Chen W, Emery S, Fritsche L, Fuchsberger C, Jun G, Li B, Lyons R, Scheller C, Sidore C, Song S, Sliwerska E, Taliun D, Tan A, Welch R, Wing MK, Zhan X, Awadalla P, Hodgkinson A, Li Y, Shi X, Quitadamo A, Lunter G, Marchini JL, Myers S, Churchhouse C, Delaneau O, Gupta-Hinch A, Kretzschmar W, Iqbal Z, Mathieson I, Menelaou A, Rimmer A, Xifara DK, Oleksyk TK, Fu Y, Liu X, Xiong M, Jorde L, Witherspoon D, Xing J, Browning BL, Browning SR, Hormozdiari F, Sudmant PH, Khurana E, Tyler-Smith C, Albers CA, Ayub Q, Chen Y, Colonna V, Jostins L, Walter K, Xue Y, Gerstein MB, Abyzov A, Balasubramanian S, Chen J, Clarke D, Fu Y, Harmanci AO, Jin M, Lee D, Liu J, Mu XJ, Zhang J, Zhang Y, Hartl C, Shakir K, Degenhardt J, Meiers S, Raeder B, Casale FP, Stegle O, Lameijer EW, Hall I, Bafna V, Michaelson J, Gardner EJ, Mills RE, Dayama G, Chen K, Fan X, Chong Z, Chen

T, Chaisson MJ, Huddleston J, Malig M, Nelson BJ, Parrish NF, Blackburne B, Lindsay SJ, Ning Z, Zhang Y, Lam H, Sisu C, Challis D, Evani US, Lu J, Nagaswamy U, Yu J, Li W, Habegger L, Yu H, Cunningham F, Dunham I, Lage K, Jespersen JB, Horn H, Kim D, Desalle R, Narechania A, Sayres MAW, Mendez FL, Poznik GD, Underhill PA, Mittelman D, Banerjee R, Cerezo M, Fitzgerald TW, Louzada S, Massaia A, Yang F, Kalra D, Hale W, Dan X, Barnes KC, Beiswanger C, Cai H, Cao H, Henn B, Jones D, Kaye JS, Kent A, Kerasidou A, Mathias R, Ossorio PN, Parker M, Rotimi CN, Royal CD, Sandoval K, Su Y, Tian Z, Tishkoff S, Via M, Wang Y, Yang H, Yang L, Zhu J, Bodmer W, Bedoya G, Cai Z, Gao Y, Chu J, Peltonen L, Garcia-Montero A, Orfao A, Dutil J, Martinez-Cruzado JC, Mathias RA, Hennis A, Watson H, McKenzie C, Qadri F, LaRocque R, Deng X, Asogun D, Folarin O, Happi C, Omoniwa O, Stremlau M, Tariyal R, Jallow M, Joof FS, Corrah T, Rockett K, Kwiatkowski D, Kooner J, Hien TT, Dunstan SJ, ThuyHang N, Fonnie R, Garry R, Kanneh L, Moses L, Schieffelin J, Grant DS, Gallo C, Poletti G, Saleheen D, Rasheed A, Brooks LD, Felsenfeld AL, McEwen JE, Vaydylevich Y, Duncanson A, Dunn M, Schloss JA. (Nature Publishing Group, 2015), vol. 526, pp. 68–74.

75. Pando MJ, Gardiner CM, Gleimer M, McQueen KL, Parham P, The protein made from a common allele of KIR3DL1 (3DL1*004) is poorly expressed at cell surfaces due to substitution at positions 86 in Ig domain 0 and 182 in Ig domain 1. J Immunol 171, 6640–6649 (2003). [PubMed: 14662867]
76. Trompeter HI, Gómez-Lozano N, Santourlidis S, Eisermann B, Wernet P, Vilches C, Uhrberg M, Three structurally and functionally divergent kinds of promoters regulate expression of clonally distributed killer cell Ig-like receptors (KIR), of KIR2DL4, and of KIR3DL3. J Immunol 174, 4135–4143 (2005). [PubMed: 15778373]
77. Chan H-W, Kurago ZB, Stewart CA, Wilson MJ, Martin MP, Mace BE, Carrington M, Trowsdale J, Lutz CT, DNA Methylation Maintains Allele-specific KIR Gene Expression in Human Natural Killer Cells. Journal of Experimental Medicine 197, 245–255 (2003). [PubMed: 12538663]
78. Li H, Pascal V, Martin MP, Carrington M, Anderson SK, Genetic Control of Variegated KIR Gene Expression: Polymorphisms of the Bi-Directional KIR3DL1 Promoter Are Associated with Distinct Frequencies of Gene Expression. PLOS Genetics 4, e1000254 (2008).
79. Li H, A statistical framework for SNP calling, mutation discovery, association mapping and population genetical parameter estimation from sequencing data. Bioinformatics 27, 2987–2993 (2011). [PubMed: 21903627]
80. Farre D, Roset R, Huerta M, Adsuara JE, Rosello L, Alba MM, Messeguer X, Identification of patterns in biological sequences at the ALGGEN server: PROMO and MALGEN. Nucleic Acids Res 31, 3651–3653 (2003). [PubMed: 12824386]
81. Van Den Broeck T, Stevenaert F, Taveirne S, Debacker V, Vangestel C, Vandekerckhove B, Taghon T, Matthys P, Plum J, Held W, Dewerchin M, Yokoyama WM, Leclercq G, Ly49E-dependent inhibition of natural killer cells by urokinase plasminogen activator. Blood 112, 5046–5051 (2008). [PubMed: 18784372]
82. Van Den Broeck T, Van Ammel E, Delforche M, Taveirne S, Kerre T, Vandekerckhove B, Taghon T, Plum J, Leclercq G, Differential *Ly49e* Expression Pathways in Resting versus TCR-Activated Intraepithelial γδ T Cells. The Journal of Immunology 190, 1982 (2013).
83. Van Acker A, Filtjens J, Van Welden S, Taveirne S, Van Ammel E, Vanhees M, Devisscher L, Kerre T, Taghon T, Vandekerckhove B, Plum J, Leclercq G, Ly49E Expression on CD8αα-Expressing Intestinal Intraepithelial Lymphocytes Plays No Detectable Role in the Development and Progression of Experimentally Induced Inflammatory Bowel Diseases. PLOS ONE 9, e110015 (2014).
84. Filtjens J, Keirsse J, Van Ammel E, Taveirne S, Van Acker A, Kerre T, Taghon T, Vandekerckhove B, Plum J, Van Ginderachter JA, Leclercq G, Expression of the inhibitory Ly49E receptor is not critically involved in the immune response against cutaneous, pulmonary or liver tumours. Scientific Reports 6, 30564 (2016). [PubMed: 27469529]
85. Van Beneden K, De Creus A, Stevenaert F, Debacker V, Plum J, Leclercq G, Expression of Inhibitory Receptors Ly49E and CD94/NKG2 on Fetal Thymic and Adult Epidermal TCR Vγ3 Lymphocytes. The Journal of Immunology 168, 3295 (2002). [PubMed: 11907085]
86. Stevenaert F, Van Beneden K, De Creus A, Debacker V, Plum J, Leclercq G, Ly49E expression points toward overlapping, but distinct, natural killer (NK) cell differentiation kinetics and

potential of fetal versus adult lymphoid progenitors. J Leukoc Biol 73, 731–738 (2003). [PubMed: 12773505]

87. Kelley J, Walter L, Trowsdale J, Comparative genomics of natural killer cell receptor gene clusters. PLoS Genet 1, 129–139 (2005). [PubMed: 16132082]
88. Rahim MM, Tu M, Mahmoud A, Wight A, Abou-Samra E, Lima P, Makrigiannis A, Ly49 Receptors: Innate and Adaptive Immune Paradigms. Frontiers in Immunology 5, (2014).
89. Swamy M, Abeler-Dörner L, Chettle J, Mahlakõiv T, Goubau D, Chakravarty P, Ramsay G, Reis e Sousa C, Staeheli P, Blacklaws BA, Heeney JL, Hayday AC, Intestinal intraepithelial lymphocyte activation promotes innate antiviral resistance. Nature Communications 6, 7090 (2015).
90. Vandereyken M, James OJ, Swamy M, Mechanisms of activation of innate-like intraepithelial T lymphocytes. Mucosal Immunology 13, 721–731 (2020). [PubMed: 32415229]
91. Tian Y, Sun Y, Gao F, Koenig MR, Sunderland A, Fujiwara Y, Torphy RJ, Chen L, Edil BH, Schulick RD, Zhu Y, CD28H expression identifies resident memory CD8 + T cells with less cytotoxicity in human peripheral tissues and cancers. Oncoimmunology 8, e1538440-e1538440 (2018).
92. McDonald BD, Jabri B, Bendelac A, Diverse developmental pathways of intestinal intraepithelial lymphocytes. Nature reviews. Immunology 18, 514–525 (2018).
93. Brenes AJ, Vandereyken M, James OJ, Watt H, Hukelmann J, Spinelli L, Dikovskaya D, Lamond AI, Swamy M, Tissue environment, not ontogeny, defines murine intestinal intraepithelial T lymphocytes. eLife 10, e70055 (2021). [PubMed: 34473623]
94. Melandri D, Zlatareva I, Chaleil RAG, Dart RJ, Chancellor A, Nussbaumer O, Polyakova O, Roberts NA, Wesch D, Kabelitz D, Irving PM, John S, Mansour S, Bates PA, Vantourout P, Hayday AC, The γδTCR combines innate immunity with adaptive immunity by utilizing spatially distinct regions for agonist selection and antigen responsiveness. Nature immunology 19, 1352–1365 (2018). [PubMed: 30420626]
95. Hwang J-R, Byeon Y, Kim D, Park S-G, Recent insights of T cell receptor-mediated signaling pathways for T cell activation and development. Experimental & Molecular Medicine 52, 750–761 (2020). [PubMed: 32439954]
96. Maeda Y, Nishikawa H, Sugiyama D, Ha D, Hamaguchi M, Saito T, Nishioka M, Wing James B, Adeegbe D, Katayama I, Sakaguchi S, Detection of self-reactive CD8+ T cells with an anergic phenotype in healthy individuals. Science 346, 1536–1540 (2014). [PubMed: 25525252]
97. Redmond WL, Sherman LA, Peripheral Tolerance of CD8 T Lymphocytes. Immunity 22, 275–284 (2005). [PubMed: 15780985]
98. Davey MS, Willcox CR, Baker AT, Hunter S, Willcox BE, Recasting Human Vδ1 Lymphocytes in an Adaptive Role. Trends in immunology 39, 446–459 (2018). [PubMed: 29680462]
99. Willcox CR, Pitard V, Netzer S, Couzi L, Salim M, Silberzahn T, Moreau J-F, Hayday AC, Willcox BE, Déchanet-Merville J, Cytomegalovirus and tumor stress surveillance by binding of a human γδ T cell antigen receptor to endothelial protein C receptor. Nature immunology 13, 872–879 (2012). [PubMed: 22885985]
100. Roy S, Ly D, Castro CD, Li N-S, Hawk AJ, Altman JD, Meredith SC, Piccirilli JA, Moody DB, Adams EJ, Molecular Analysis of Lipid-Reactive Vδ1 γδ T Cells Identified by CD1c Tetramers. The Journal of Immunology, 1502202 (2016).
101. Li J, Zaslavsky M, Su Y, Guo J, Sikora MJ, van Unen V, Christophersen A, Chiou SH, Chen L, Li J, Ji X, Wilhelmy J, McSween AM, Palanski BA, Mallajosyula VVA, Bracey NA, Dhondalay GKR, Bhamidipati K, Pai J, Kipp LB, Dunn JE, Hauser SL, Oksenberg JR, Satpathy AT, Robinson WH, Dekker CL, Steinmetz LM, Khosla C, Utz PJ, Sollid LM, Chien YH, Heath JR, Fernandez-Becker NQ, Nadeau KC, Saligrama N, Davis MM, KIR(+)CD8(+) T cells suppress pathogenic T cells and are active in autoimmune diseases and COVID-19. Science 376, eabi9591 (2022). [PubMed: 35258337]
102. Kim HJ, Wang X, Radfar S, Sproule TJ, Roopenian DC, Cantor H, CD8+ T regulatory cells express the Ly49 Class I MHC receptor and are defective in autoimmune prone B6-Yaa mice. Proc Natl Acad Sci U S A 108, 2010–2015 (2011). [PubMed: 21233417]
103. Anfossi N, Robbins SH, Ugolini S, Georgel P, Hoebe K, Bouneaud C, Ronet C, Kaser A, DiCioccio CB, Tomasello E, Blumberg RS, Beutler B, Reiner SL, Alexopoulou L, Lantz O,

Raulet DH, Brossay L, Vivier E, Expansion and function of CD8+ T cells expressing Ly49 inhibitory receptors specific for MHC class I molecules. J Immunol 173, 3773–3782 (2004). [PubMed: 15356124]

104. Swainson LA, Mold JE, Bajpai UD, McCune JM, Expression of the autoimmune susceptibility gene FcRL3 on human regulatory T cells is associated with dysfunction and high levels of programmed cell death-1. J Immunol 184, 3639–3647 (2010). [PubMed: 20190142]
105. Bryceson YT, March ME, Ljunggren HG, Long EO, Synergy among receptors on resting NK cells for the activation of natural cytotoxicity and cytokine secretion. Blood 107, 159–166 (2006). [PubMed: 16150947]
106. Norman PJ, Hollenbach JA, Nemat-Gorgani N, Marin WM, Norberg SJ, Ashouri E, Jayaraman J, Wroblewski EE, Trowsdale J, Rajalingam R, Oksenberg JR, Chiaroni J, Guethlein LA, Traherne JA, Ronaghi M, Parham P, Defining KIR and HLA Class I Genotypes at Highest Resolution via High-Throughput Sequencing. Am J Hum Genet 99, 375–391 (2016). [PubMed: 27486779]
107. Li H, Durbin R, Fast and accurate short read alignment with Burrows-Wheeler transform. Bioinformatics 25, 1754–1760 (2009). [PubMed: 19451168]
108. Hadfield JD, MCMC methods for multi-response generalized linear mixed models: the MCMCglmm R package. Journal of statistical software 33, 1–22 (2010). [PubMed: 20808728]
109. Miah SMS, Campbell KS, Expression of cDNAs in human Natural Killer cell lines by retroviral transduction. Methods Mol Biol 612, 199–208 (2010). [PubMed: 20033642]
110. Sork H, Nordin JZ, Turunen JJ, Wiklander OP, Bestas B, Zaghloul EM, Margus H, Padari K, Duru AD, Corso G, Bost J, Vader P, Pooga M, Smith CE, Wood MJ, Schiffelers RM, Hällbrink M, Andaloussi SE, Lipid-based Transfection Reagents Exhibit Cryo-induced Increase in Transfection Efficiency. Mol Ther Nucleic Acids 5, e290–e290 (2016). [PubMed: 27111416]
111. Aricescu AR, Lu W, Jones EY, A time- and cost-efficient system for high-level protein production in mammalian cells. Acta Crystallogr D Biol Crystallogr 62, 1243–1250 (2006). [PubMed: 17001101]
112. Fang XT, Sehlin D, Lannfelt L, Syvanen S, Hultqvist G, Efficient and inexpensive transient expression of multispecific multivalent antibodies in Expi293 cells. Biol Proced Online 19, 11 (2017). [PubMed: 28932173]
113. Litwin V, Gumperz J, Parham P, Phillips JH, Lanier LL, NKB1: a natural killer cell receptor involved in the recognition of polymorphic HLA-B molecules. J Exp Med 180, 537–543 (1994). [PubMed: 8046332]
114. Soderstrom K, Corliss B, Lanier LL, Phillips JH, CD94/NKG2 is the predominant inhibitory receptor involved in recognition of HLA-G by decidual and peripheral blood NK cells. J Immunol 159, 1072–1075 (1997). [PubMed: 9233599]
115. Estefania E, Flores R, Gomez-Lozano N, Aguilar H, Lopez-Botet M, Vilches C, Human KIR2DL5 is an inhibitory receptor expressed on the surface of NK and T lymphocyte subsets. J Immunol 178, 4402–4410 (2007). [PubMed: 17371997]

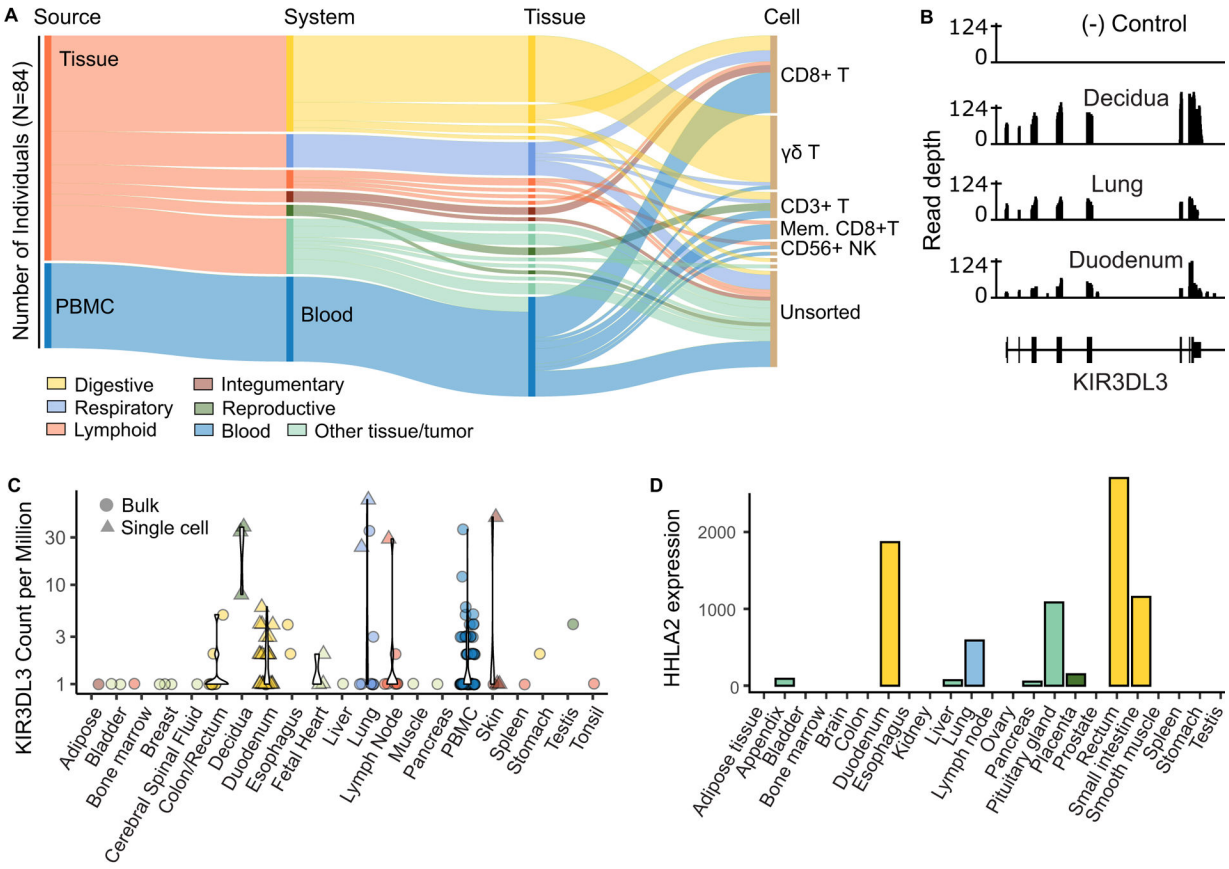

Figure 1: KIR3DL3 mRNA identified in PBMCs and tissues that express HHLA2.

(A) Shown are the frequency of tissue source, systems, tissues, and sorted cell types of 84 individuals identified from 360,787 short read archive records as having KIR3DL3 transcripts. (B) All sequence reads from three KIR3DL3+ samples were mapped to the hg38 human genome reference. Each sample showed high depth of coverage across KIR3DL3 exons. (C) Plotted is the frequency of the KIR3DL3 subsequence per million reads. Colors indicate tissue system, symbols indicate bulk (circles) or single-cell (triangles) RNA sequencing experiments. (D) HHLA2 protein expression as described (44), colors indicate tissue system.

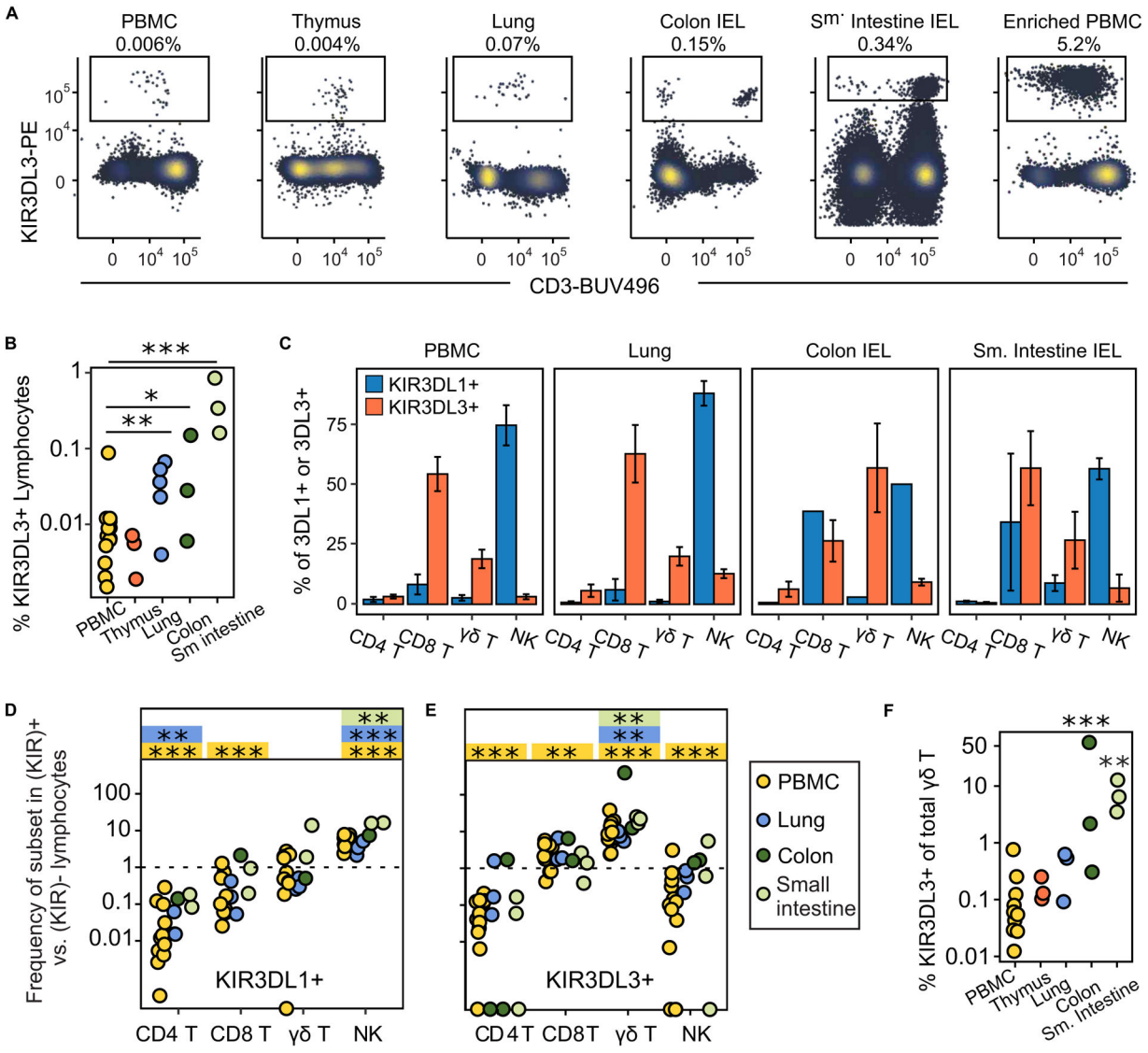

Figure 2: KIR3DL3 is enriched in CD8+ and γδ T cells of PBMC, lung, and digestive tract IELs.

Human PBMCs, thymocytes, lung lymphocytes, and digestive tract intra-epithelial lymphocytes (IELs) analyzed using 17-color spectral flow cytometry. (A) Shown is the percentage of cells expressing KIR3DL3 in the viable CD14-CD19- population, isolated from the tissue indicated at the top each panel. (B) Summary of (A) across ten PBMC, three thymi, five lung, three colon, and three small intestine donors. (C-E) Magnetic bead enrichment (e.g. Enriched PBMC) was used to increase the number of KIR3DL3+ cells prior to flow cytometry. (C) The percentage of CD4+ T, CD8+ T, γδ T, and NK cells was calculated for KIR3DL1+CD19- and KIR3DL3+CD19- lymphocytes. These frequencies (C) were compared to the background (CD19-) to determine the enrichment of KIR3DL1 and KIR3DL3 expression in CD4+ T, CD8+ T, γδ T, and NK cells (D-E). Significant differences in the frequency of lymphocyte subsets within CD19- and KIR+CD19- parent populations are indicated, with asterisks in boxes colored by tissue. (F) Shows the proportion of

γδ T cells that express KIR3DL3 according to the tissue of origin. *p<0.05, **p<0.01, ***p<0.001

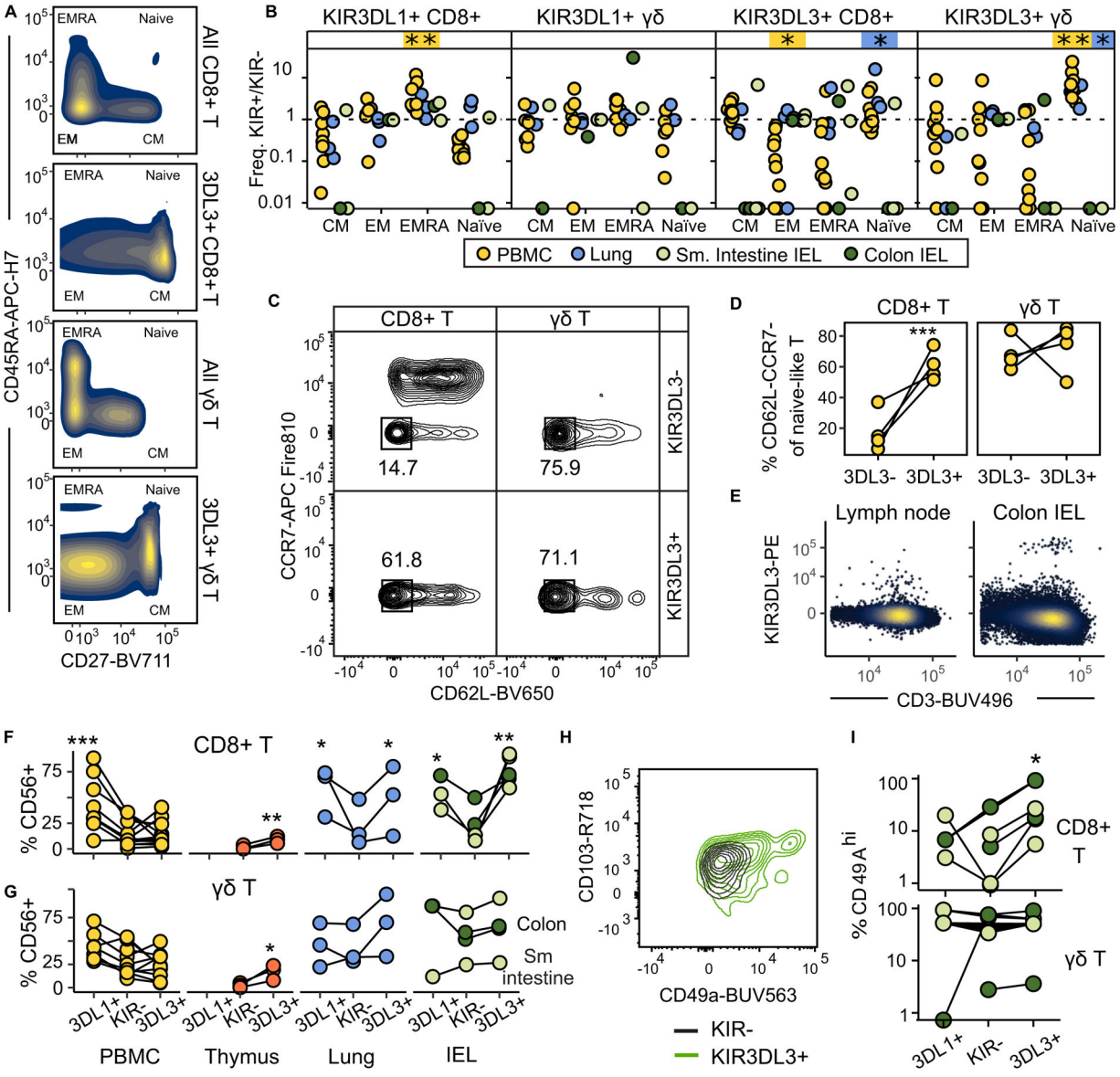

Figure 3: KIR3DL3+ T cells can co-express naïve, innate, and tissue-resident T cell markers.

(A) Distribution of CD27 and CD45RA on CD8+ T or γδ T cells unselected (upper) or selected (lower) for KIR3DL3 expression. Average kernel density across five PBMC donors is shown. EM=effector memory, EMRA=EM re-expressing CD45RA, CM=central memory. (B) Frequency of CM-, EM-, EMRA-, and naïve-like CD8+ or γδ T cell populations in KIR3DL1+ or KIR3DL3+ cells were divided by the frequency of these populations in KIR3DL1- or KIR3DL3- cells. (C) The expression profile of CCR7 and CD62L within naïve-like (CD45RA+CD27+) CD8+ and γδ T cells from PBMC was plotted according to KIR3DL3 expression. Box indicates % of CD62L-CCR7-. (D) Shows the proportion of CD62L-CCR7- double negative T cells across 4 donors. (E) KIR3DL3 expression in IELs from colon tissue and a nearby colon-associated lymph node. (F) The proportion of cells expressing CD56 on KIR-, KIR3DL1+, or KIR3DL3+ CD8+ T or (G) γδ T cells. Each line represents one donor. (H) Representative contour plot of CD49a^{hi} population on KIR3DL3+

CD8+ T cells from the intestine. (I) The summarized proportion of CD49hi cells of 3DL1+, KIR-, or 3DL3+ CD8+ and γδ T cells. *p<0.05, **p<0.01, ***p<0.001 by linear mixed models.

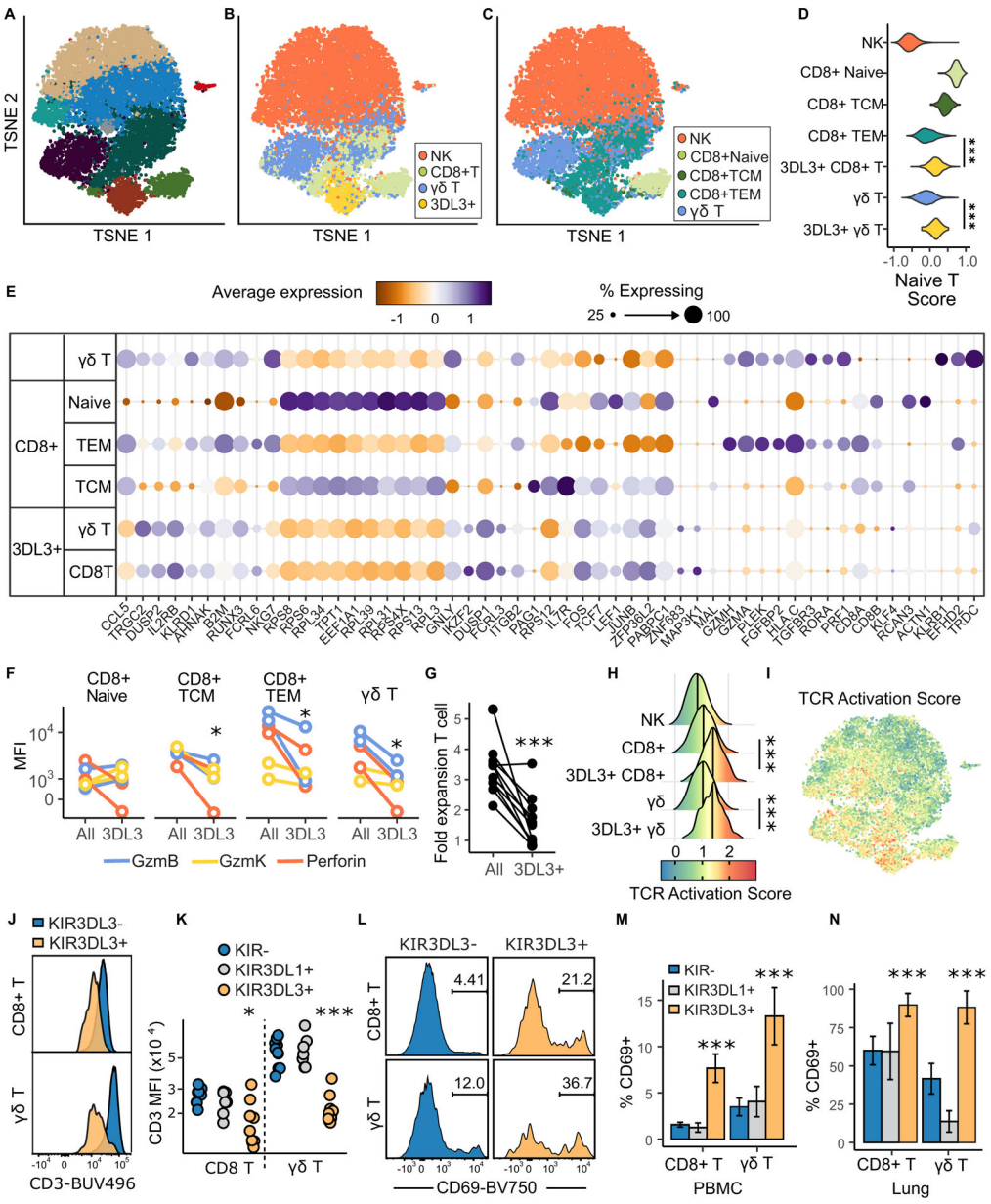

Figure 4: KIR3DL3+ cells are hypofunctional with a signature of recent TCR activation.

(A-C) Single cell RNA sequencing of sorted NK, CD8+ T, γδ T, and KIR3DL3+ cells from PBMC of 5 donors; visualized using TSNE, colored according to Seurat cluster (A), sorted population (B), or by T cell subpopulation as assigned by multimodal reference mapping (C). (D) VISION derived Naïve T Score, using genes that defined CD8+ naïve T cells in our data. (E) KIR3DL3+ cells in each T cell subpopulation (from panel (C)) compared to respective KIR3DL3- populations for differential gene expression testing in Seurat. Dot plots show the percentage of cells expressing each gene (named underneath) and the average scaled expression within each subpopulation. (F) PBMC from 2 donors stained for GzmB, GzmK, and Perforin. (G) PBMC stimulated with T Cell-Activator dynabeads. Shown is fold expansion of all T cells and KIR3DL3+ T cells per donor (n=11). (H-I) VISION derived

T Cell Activation score (Fig. S8 for gene list), plotted as the distribution of the score of each cell across cell subsets (H) or by color on the TSNE dimension reduction (I). (J) Representative histograms of CD3 expression on KIR3DL3- (blue) or KIR3DL3+ (orange) CD8+ T cells (upper panel) and γδ T cells (lower panel) from PBMCs. (K) MFI of CD3 expression on KIR- (blue), KIR3DL1+ (grey) and KIR3DL3+ (orange) CD8+ T cells or γδ T cells (n= 10 PBMC donors). (L) Representative histograms showing the proportion of CD69+ KIR3DL3- (blue) or KIR3DL3+ (orange) on CD8+ T cells (upper panel) and γδ T cells (lower panel) from PBMCs and summarized in (M) PBMC (n=10) and (N) lungs (n=3). *p<0.05, **p<0.01, ***p<0.001 by linear mixed models.

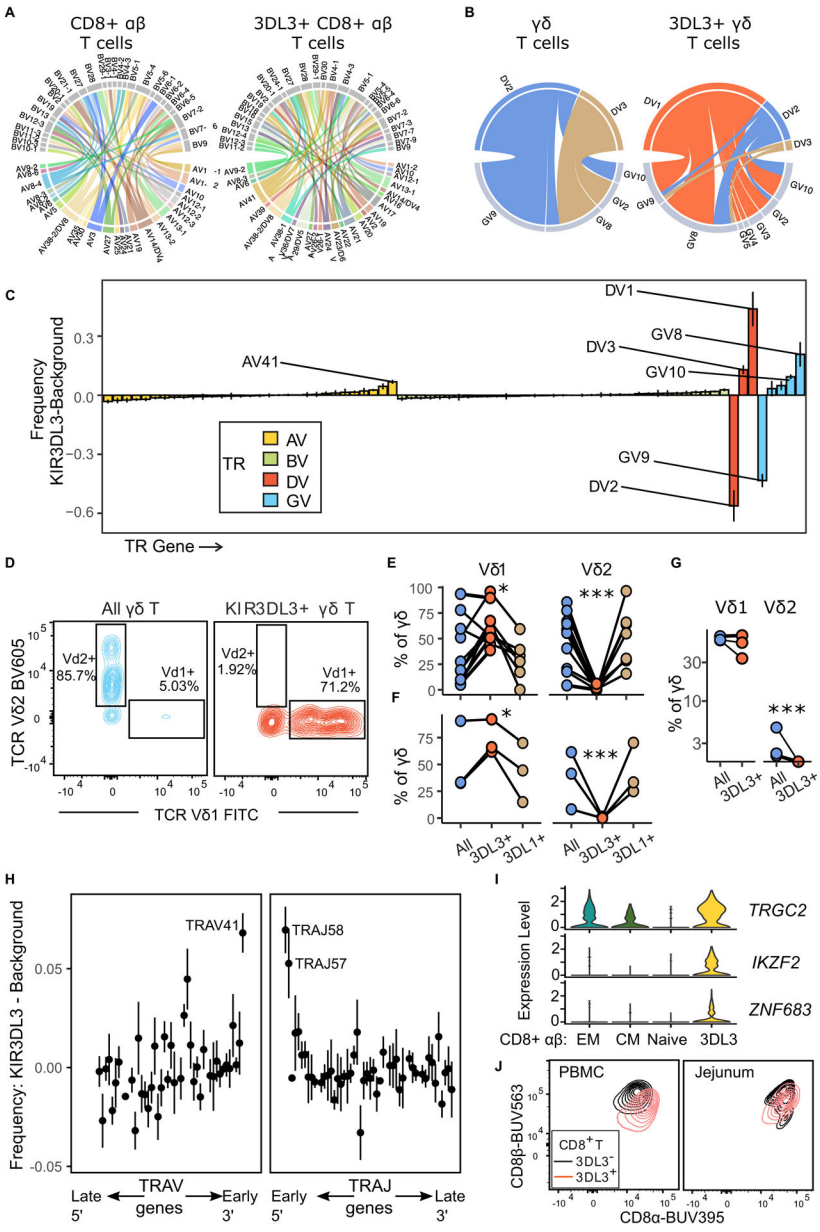

Figure 5: KIR3DL3 is preferentially expressed on T cells utilizing Vδ1 or early rearranged α chain TCRs.

Single cell paired αβ or γδ TCR sequencing of PBMCs from five individuals following sorting for KIR3DL3+, total γδ, or CD8+ αβ T cells. (A-B) Representative Circos plots of paired TCR variable α (TRAV) and β (TRBV) chain usage, (A) or variable γ chain (TRGV) and variable δ chain (TRDV) pairings (B) from a single donor. Each segment represents paired TCRαβ or TCRγδ usage, and the thickness of each segment reflects the frequency of the paired usage; segments are colored according to the corresponding TRAV or TRDV usage. (C) V gene usage is summarized across 5 donors by subtracting the frequency of each V gene in KIR3DL3+ cells by that in KIR3DL3- cells. Variable genes significantly associated with KIR3DL3 expression are labelled. (D) Representative contour plots of PBMCs stained with fluorescent-conjugated Vδ1 and Vδ2 antibodies and analyzed

by flow cytometry, the proportion of Vδ1+ and Vδ2+ cells are shown of total γδ T cells or KIR3DL3+ γδ T cells. Plotted are the proportions of Vδ1 and Vδ2 cells of total γδ, KIR3DL1+ γδ, and KIR3DL3+ γδ T cells across 9 PBMC (E), 3 lung (F), and 3 thymus donors (G). (H) Enrichment of TRAV and TRAJ usage in KIR3DL3+ T cells was plotted according to the propensity for each gene to undergo early TCR-α chain rearrangement (TRAV ranked 3'→ 5'; TRAJ 5' → 3'). (I) Violin plots showing gene expression levels for: TCR gamma chain (*TRGC2*), Helios (*IKZF2*), and Hobit (*ZNF683*) CD8+ αβTCR effector memory (EM), central memory (CM), naive and 3DL3 clusters. (J) Peripheral blood and jejunum intra-epithelial CD8+ T cells were stained with fluorescent CD8α and CD8β antibodies and expression detected by flow cytometry. Significance assessed by linear mixed models. *p<0.05, **p<0.01, ***p<0.001

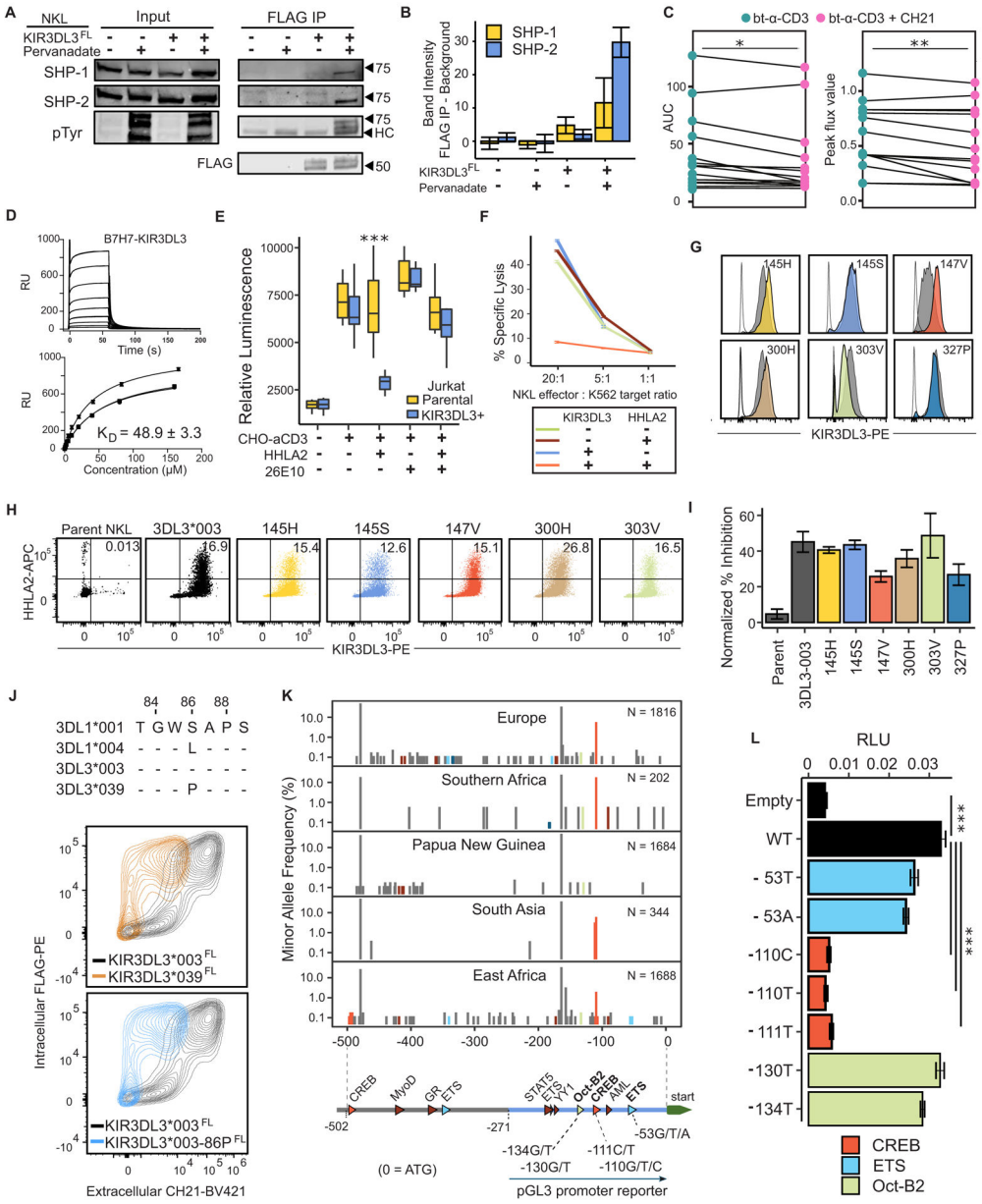

Figure 6: KIR3DL3 is an inhibitory receptor with functional polymorphism.

(A) Western blot of pervanadate-treated wild-type NKL (–) or NKL-KIR3DL3*003^{FLAG} (+) cells immunoprecipitated (IP) with anti-FLAG and stained with pTyr, FLAG, SHP-1, SHP-2, or β-tub specific antibodies. HC = heavy chain contamination from IP. (B) SHP-1 and SHP-2 quantified as band intensity (relative to background) following FLAG IP, divided by band intensity of input (n = 3). (C) Relative calcium flux of Jurkat-9C2-KIR3DL3 cells with biotinylated anti-CD3 (bt-αCD3) with or without biotinylated anti-KIR3DL3 (bt-αKIR3DL3) and following avidin crosslinking. AUC = baseline-corrected area under the curve. Shows 7 independent experiments with 2–3 replicates each. (D) SPR of HHLA2 vs. KIR3DL3. Top: Sensorgrams. Bottom: Affinity curves, from two independent experiments with two replicates each (RU=response units). (E) NFAT activity of Jurkat and Jurkat-

KIR3DL3 reporter cells co-cultured with CHO stimulator cells +/− HHLA2 expression. 26E10 = KIR3DL3 blocking mAb (F) Lysis of K562 targets (+/− HHLA2) by NKL effectors (+/− KIR3DL3). (G,H,I) KIR3LD3*003 allotype compared to 6 naturally-selected amino acid variants. (G) KIR3DL3-PE staining for parental NKL (empty), NKL-KIR3DL3*003 (grey) and NKL expressing each variant. (H) Staining for KIR3DL3 and Fc, following incubation with HHLA2-Fc (I) Shows percent inhibition (721.221-HHLA2 vs 721.221) of NKL cytotoxicity for each variant (ET 20:1, n=3). (J) (upper) Residue 86 polymorphism defines KIR3DL1*004 and KIR3DL3*039. (lower) For 293T cells expressing FLAG-tagged KIR3DL3 variants; extracellular and intracellular KIR3DL3 expression was determined using CH21 and anti-FLAG, respectively. (K) Shows minor allele frequencies (upper) and their location in transcription factor sites (lower), of any nucleotide variants identified within 500 bp of the KIR3DL3 start codon, in 5 populations. (L) Ratio of firefly to renilla luciferase (relative light units; RLU) of 8 proximal promoter variants in pGL3 transfected 293T cells. *p<0.05, **p<0.01, ***p<0.001 by linear mixed models.